Drug Development and Industrial Pharmacy, 2012; 38(3): 271–293

ISSN 0363-9045 print/ISSN 1520-5762 online
DOI: 10.3109/03639045.2011.598538

informa
healthcare

RESEARCH ARTICLE

Advanced preformulation investigations for the development of a lead intravaginal bioadhesive polymeric device

Valence M. K. Ndesendo[1], Viness Pillay[1], Yahya E. Choonara[1], Lisa C. du Toit[1], Eckhart Buchmann[2], Pradeep Kumar[1], Riaz A. Khan[3], and Leith C.R. Meyer[4]

[1]University of the Witwatersrand, Department of Pharmacy and Pharmacology, Parktown, Johannesburg, South Africa, [2]Chris Hani Baragwanath Hospital, Department of Gynaecology and Obstetrics, Bertsham, Johannesburg, South Africa, [3]Manav Rachna International University, Aravali Hills, Faridabad, India, and [4]University of the Witwatersrand, Central Animal Services, Parktown, Johannesburg, South Africa

Abstract

Context and Objective: To screen various polymers through extensive preformulation investigations to ultimately obtain a lead polymer combination for designing a desirable Intravaginal Bioadhesive Polymeric Device (IBPD).

Materials and methods: Hydrophilic and hydrophobic polymers (18) at different combinations were blended and compressed into 62 caplet-shaped devices at 5 tons, one of the hydrophilic polymers being a modified synthetic product of polyamide 6,10 ($_m$PA 6,10). Two sets of crosslinked PAA-based caplets comprising either allyl-sucrose (AS-PAA) or allyl-penta-erythritol (APE-PAA) were explored. The devices were subjected to in-process validation tests and thereafter to preformulation investigational screening {equilibrium swelling ratio (ESR) being a screening parameter}, using a One Variable at a Time (OVAT) approach. Molecular mechanics force field simulations in both vacuum and solvated systems were conducted to investigate the influence of addition and subsequent replacement of a polymer(s) on the spatial disposition and energetic profile of the sterically constrained and geometrically optimized multi-polymeric complex, IBPD.

Results and discussion: The developed devices were sufficiently strong (longitudinal crushing force:286 ± 0.01 N; mean weight:600 ± 0.48 mg; mean friability:0.31 ± 0.04%). Through OVAT approach, 15 lead formulations with minimal swelling tendencies (ESRs ranging from 0.011 to 0.084) were obtained out of 62 formulations. F62 {i.e. $_m$PA 6,10, (150 mg), PLGA (400 mg), EC (200 mg), PVA (25 mg) and PAA (25 mg)} displayed minimal swelling tendency and therefore the highest stability. The highly stabilized conformation of the final *in silico* IBPD polymeric assembly PLGA-$_m$PA6,10-PVA-PAA-EC corroborated the experimental results in terms of preformulation investigational screening using the OVAT approach.

Conclusion: The results obtained suggest that $_m$PA 6,10, PLGA, EC, PVA and PAA at an appropriate weight ratio may be suitable for development of an IBPD.

Keywords: Equilibrium swelling ratio (ESR), intravaginal bioadhesive polymeric device (IBPD), preformulation investigations, matrix stability, OVAT

Introduction

Major efforts have been directed toward designing intravaginal drug delivery systems that can deliver drugs to the vagina at a desired rate to maximize drug efficacy while minimizing side effects[1–4]. However, successful design of intravaginal drug delivery systems still poses numerous challenges[5–7]. It is imperative that the type and properties of the drug and the drug carrier (e.g. polymer) be thoroughly understood if successful intravaginal delivery is to be achieved. In the case of a polymer as the carrier agent, appropriate selection is of paramount importance. The polymer employed can be either degradable or non-degradable. Biodegradable polymers that are biocompatible to the body are most frequently chosen

Address for Correspondence: Viness Pillay, University of the Witwatersrand, Department of Pharmacy and Pharmacology, Parktown, Johannesburg, South Africa. Tel: +27-11-717–2274, Fax: +27-11-642–4355. E-mail: viness.pillay@wits.ac.za

(Received 17 March 2011; revised 30 May 2011; accepted 15 June 2011)

for the design of intravaginal drug delivery systems. Their value is attributed to the fact that they do not require to be removed from the body after application. The type, physicochemical and physicomechanical properties, proportions of the polymers in the formulation, as well as the degree of swelling and/or erosion for the polymers employed in formulating an intravaginal delivery system, play an important role in matrix integrity and retention capacity[8]. These are the determinant factors for bioadhesion and release characteristics of a given system[9,10]. A polymer's physicochemical and physicomechanical properties contribute substantially to diffusion, swelling, degradation and erosion dynamics, which play an important role in terms of drug release kinetics[11–13]. Other phenomena such as osmotic, magnetic or electric effects may also be involved. The chemical nature of polymers commonly used for pharmaceutical purposes differs significantly. Some are freely water-soluble, while others are completely water-insoluble. Thus, they vary in the rate and extent of swelling, bioerosion/biodegradation and their potential to interact with the drug.

In the current study, both natural and synthetic biodegradable and biocompatible polymers have been employed, some with hydrophilic properties, others with hydrophobic properties and yet others with bioadhesion properties. Hydrophilic polymers can control drug release because of their compressibility and swelling properties, as well as the ability to accommodate high levels of drugs[14–16]. However, hydrophilic matrix systems generally result in nearly first-order release profiles[17–19]. For this reason, use of both hydrophilic and hydrophobic polymers have been considered to be an absolute necessity in this study since the ultimate aim was to achieve zero-order delivery[20–22]. Studies have shown that an increase in hydrophobicity may substantially alter the release kinetics of a drug delivery system[23–26]. This is attributable to its ability to hinder the penetration of the solvent molecules into the polymer matrix thereby leading to a reduction in the drug release rate[27–29]. Furthermore, an increase in hydrophobicity often assists to control the rate of polymer disentanglement[24,26]. This occurs through various mechanisms, but mostly through a decreased tendency for the polymer to undergo hydrolysis due to decreased exposure to water[24–26,30]. In addition, hydrophobilic polymers may also provide several advantages, ranging from differing stability at varying pH and moisture levels, to well-established safe applications[31].

In this study a novel caplet-shaped device was considered to be the most appropriate based on the route of application. Conventional vaginal delivery systems including solutions, semi-solids (ointments, creams, gels), tablets and pessaries suffer in one way or another from the problems of retention, spreadability and drug release control[1,2,32]. Semi-solids in particular are perceived as messy in use and prone to leakage[5,33]. Furthermore, the conventional vaginal drug delivery systems do not provide sufficient design flexibility in the control of drug release over periods extending from days to months. In this regard, there is then a great need for designing more specific formulations that can circumvent the problems associated with the conventional vaginal drug delivery systems.

Polymer swelling is one of the factors that determines the matrix stability and subsequently the drug release kinetics from polymer matrices[34–36]. Normally in swellable polymer matrices, polymer relaxation and erosion mechanisms may coexist[37]. Swelling and erosion front domains specifically define the gel layer thickness, which is considered to be the key factor in drug release kinetics and in most cases occur simultaneously[37–39]. Thus, the extent of polymer swelling, relative mobilities of dissolution medium and drug, and matrix erosion dictate the kinetics as well as mechanism of drug release from polymeric matrices[40]. Generally, swelling–controlled release systems consist of a drug, which is molecularly dispersed in a polymeric matrix. Swelling occurs with subsequent formation of a thin gel layer as soon as water begins to penetrate the polymer matrix. In addition, it has been shown that the porosity of a polymeric system is another dominant factor that may control the swelling behavior[41,42]. Increased porosity leads to fast initial rates of water uptake and therefore high extent of swelling equilibrium. For a better outcome in terms of matrix stability and therefore optimal drug release kinetics, low swelling and slow erosion are the most desirable features.

The aim of this study was therefore to screen various polymers through an extensive preformulation investigation so as to ultimately obtain polymer combinations for the design of a lead Intravaginal Bioadhesive Polymeric Device (IBPD). A one-dimensional search with successive variation in variables i.e. OVAT approach was employed following a pre-pivoted experimental design. Although it is practically impossible for a one-dimensional search to accomplish an appropriate optimum in a finite number of experiments[43,44], it does successfully provide a lead formulation/s upon which mathematical optimization can be used for further refinement. Thus, a series of swelling tests were conducted on 62 formulations that were derived from 18 polymers, to investigate which formulation had the optimal swelling at both simulated and seminal vaginal fluids. The swelling behavior was determined in terms of the equilibrium swelling ratio (ESR) which was the critical indicator of the formulation's matrix stability (i.e. the degree of matrix robustness), and was used as a screening parameter for each formulation. Chemometric modeling and Molecular mechanics (MM) force field simulations both in vacuum and solvated systems were conducted to corroborate the experimental results of the optimized multi-polymeric complex, IBPD.

Materials and methods

Materials

The following polymers were employed in this study: Modified polyamide 6,10 ($_{m}$PA 6,10) was synthesized using hexamethylenediamine, sebacoyl chloride,

anhydrous n-hexane and cyclohexane, all purchased from Sigma-Aldrich Chemie (Steinheim, Germany). The remainder of the polymers employed were commercially available. These were: poly(acrylic acid) (Carbopol® 734 and 974) (Noveon Inc., Cleveland, OH), carageenan (Type one-kappa and alpha), ethylcellulose (Ethocel-10), xanthan gum, tragacanth, bovine serum albumin (BSA) (Sigma-Aldrich Chemie), poly(ethylene oxide) (Union Carbide Corporation, Danbury, CT), poly(lactic-co-glycolic) acid (Resomer® RG504; Boehringer Ingelheim, Ingelheim, Germany), poly(vinyl alcohol), polyvinyl povidone (Merck-Schuchardt, Hohenbrunn, Germany), gelatin, beeswax (Saarchem (Pty) Ltd., Krugersdorp, South Africa), methylcellulose, hydroxyethylcellulose, hydroxypropylcellulose, hydroxypropylymethylce-llulose (Merck-Schuchardt®), poly(ethyl acrylate, methyl-methacrylate, and chlorotrimethyl-ammoniumethylmethacrilate) S 100 (Eudragit® S-100) and poly(ethyl acrylate, methylmethacrylate, and chlorotrimethyl-ammoniumethylmetha-cyrlate) RS 100 (Eudragit® RS-100) (Rohm & Co., Pharma Polymers, Darmstadt, Germany), calcium hydroxide, glycerol, acetic acid (Associated Chemical Enterprises (Pty) Ltd., Southdale, South Africa). All other reagents used were of analytical grade and employed as received.

Synthesis of modified polyamide 6,10

The modified polyamide 6,10 ($_m$PA 6,10) was synthesized in our laboratory using a method developed by Kolawole and co-workers[45] employing hexamethylenediamine (HMD), sebacoyl chloride (SC), hexane (HXN), cyclohexane (C-HXN), sodium hydroxide (NaOH) and deionized water (DW). The overall chemical reaction is illustrated in Figure 1. These researchers focused on exploring the effect of volume ratio, stoichiometric variations and the addition of solvent phase modifiers such as sodium hydroxide and cyclohexane on the physicochemical and physicomechanical properties of the $_m$PA 6,10. In the present study, it is only the optimized $_m$PA 6,10 that was synthesized. Briefly two sets of solutions were prepared. The first solution comprised SC dissolved in a mixture of HXN and C-HXN while the second solution comprised of specific quantities HMD and NaOH dissolved in DW. The optimized formulation comprised of HMD (1.5 g), SC (0.63), HXN (40 mL), C-HXN (40 mL), NaOH (0.1 g) and DW (10 mL). The first solution was gradually added to the second to form two immiscible phases which resulted in a polymeric film being formed at the interface (i.e. by an interfacial polymerization process). The polymeric film was collected as a mass by slowly rotating a glass rod at the interface. Upon collection of the polymeric mass, it was thoroughly washed, with HXN to remove any unreacted SC and then with DW (3 × 300 mL) to remove any un-reacted NaOH. The polymeric mass was then lightly rolled on filter paper (diameter 110 mm, pore size 20 μm) to remove any excess solvent and dried to a constant weight at 40°C over 48 h.

Methods

Selection of formulation components

In polymeric drug delivery systems, controlled drug delivery occurs when a polymer, whether natural or synthetic, is combined with a drug or other bioactive agent in such a manner that the bioactive agent is released from the polymeric material in a pre-determined manner. Initially 18 polymers were investigated. These were modified polyamide 6,10 ($_m$PA 6,10), poly(lactic-co-glycolic acid) (PLGA), polyethylene oxide (PEO), poly(acrylic acid) (PAA), carrageenan (CG), ethycellulose (EC), polyvinylalcohol (PVA), polyvinyly polidone (PVP), tragacanth (TG), xanthan gum (XG), gelatin (GL), methylcellulose (MC), Hydroxyethylcellulose

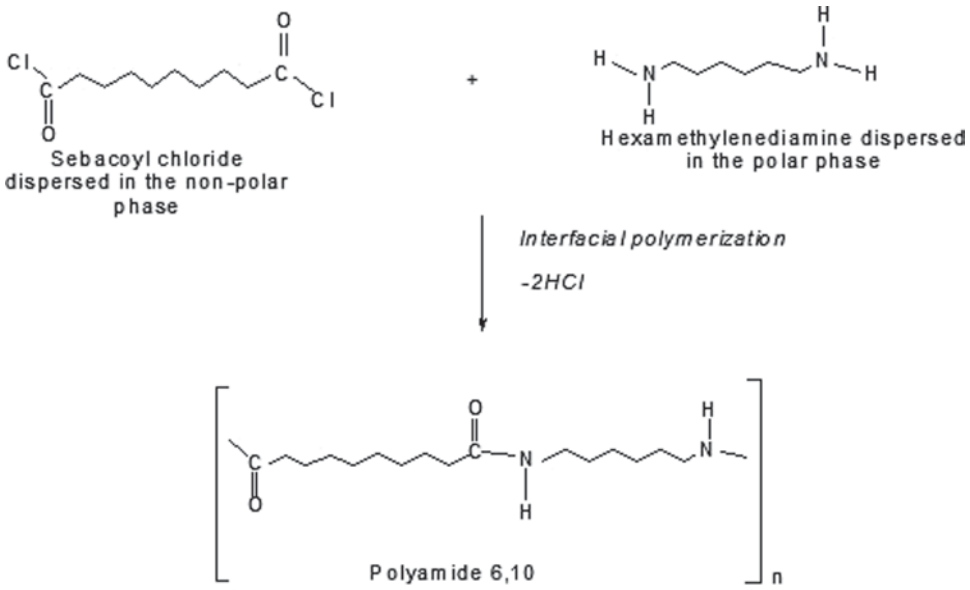

Figure 1. Synthesis of modified polyamide 6,10 by interfacial polymerization.

(HEC), hydroxypropylcellulose (HPC), hydroxypropymethylcellulose (HPMC), beeswax (BWX), poly(ethyl acrylate, methyl-methacrylate, and chlorotrimethylammoniumethylmethacrilate) S 100 (Eudragit® S100) (ED-S100) and poly(ethyl acrylate, methyl-methacrylate, and chlorotrimethyl-ammoniumethylmethacrilate) RS 100 (Eudragit® RS 100) (ED-RS100). Out of the 18 polymers, 5 of them namely modified polyamide 6,10 ($_m$PA 6,10), poly(lactic-co-glycolic acid) (PLGA), ethycellulose (EC), polyvinylalcohol (PVA) and poly(acrylic acid) (PAA) have finally been employed to encapsulate PSS and AZT (Figure 2) with the purpose of attaining controlled release within the vagina. These polymers have their own inherent properties when used alone. However, this study has aimed at using their combination, a move that is expected to provide superior physicochemical and physicomechanical properties suitable for development of the IBPD. Furthermore, these polymeric materials are FDA approved and are biocompatible and biodegradable. Table 1 depicts the polymer type, properties and the rationale for selection of each polymer.

For an intravaginal drug delivery system to be effective as an anti-HIV microbicidal agent, the drug employed should be able to inactivate HIV replication in lymphocytes, epithelial cells and sperm cells[46]. Given the fact that the passage of HIV-infected mononuclear cells in semen contributes to the sexual transmission of HIV[46,47], the anti-HIV microbicide should be metabolized with equal efficiency by both the seminal cells and the epithelial cells of the cervico-vaginal region[46]. AZT (Figure 2a) is one such a compound and therefore the reason for being employed in this study. It undergoes intracellular hydrolysis yielding monophosphate derivatives which further become phosphorylated by thymidylate kinase to produce a bioactive triphosphate derivative. PSS (Figure 2b) is a microbicidal polymer which is also homogenous and viscous, and forms bioadhesive dispersion itself, thus facilitating its retention in the vagina for prolonged periods of time[48]. Furthermore, It has been FDA approved as an alternative vaginal topical microbicide following the drawbacks found with the Nonoxynolol-9 when it was once used as a spermicidal and contraceptive (i.e. it potentiated bacterial vaginosis as well as HIV transmission[49–52]). In addition, PSS has been shown to possess some ARV effect[52], and it has gelling properties which may help in preventing HIV transmission by acting as a physical barrier

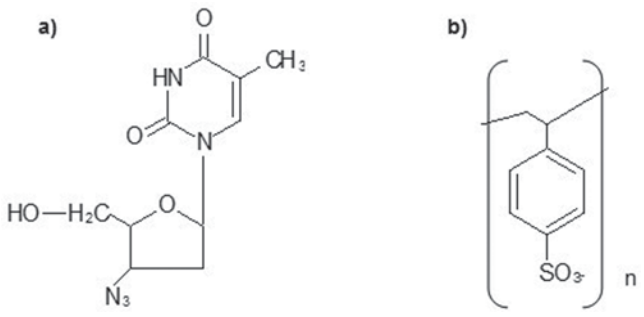

Figure 2. a) 3′-azido-3′-deoxythymidine (AZT), molecular weight 267.24 g/mol and a solubility 20.1 mg/mL, b) polystyrene Sulfonate (PSS) molecular weight 70,000 g/mol, water soluble.

Preparation of preliminary lead intravaginal bioadhesive polymeric devices

In the search for a suitable combination of polymers which will finally have the suitable bioadhesivity, matrix integrity and controlled release effect for the development of a novel controlled release intravaginal bioadhesive device, vast *in vitro* preformulation work was carried out on 18 different polymers. From these polymers, 62 different formulations weighing 800 mg each were obtained through different polymer combinations at varying quantities of each polymer (Table 2). All polymer combinations were thoroughly blended using an Erweka cube blender (Erweka Apparatebau, Heusenstamm, Germany) and then directly compressed into caplet devices using a Carver Press (Carver Inc., Hydraulic Laboratory Press, Wabash, IN) at a force of 5 tons. Each device was subjected to in-process validation tests that involved longitudinal crushing force, friability and mass uniformity analysis to ensure manufacturing reproducibility. A sample of 10 devices from each formulation was used for each test. Longitudinal crushing force test was conducted on a Hardness Tester (Pharma Test,

Table 1. Polymers, properties and rationale for selection.

Polymer	Properties	Rationale for selection
$_m$PA 6,10	• High matrix resilience • Abrasion resistance • Chemical inertness • High modulus • Thermoplasticity	• To control drug release • To control permeation • To intensify the robustness of the IBPD
PLGA	• Highly hydrophobic • Degrades into two acidic units namely lactic acid and glycolic acid	• To produce an acidic pH environment within the vagina upon degrading into lactic and glycolic acid. • Acidic pH maintains the normal vaginal ecology by favoring the growth of *Lactobacilli*-containing microflora which prevents bacterial vaginosis. • To control drug release
EC	• Highly hydrophobic • Easily compressible	• To control drug release • To control permeation
PVA	• Hydrophilic • Compressible • Mildly bioadhesive	• To control drug release • To foster bioadhesivity
PAA	• Hydrophilic • Possesses hydrogen bonds and strong anionic/ cationic charges • High molecular mass and chain flexibility • Surface energy interactions favoring spreading onto mucus	• Confers bioadhesiveness to the IBPD, thus favoring extension of drug residence time in the vagina • To control drug release • To control permeation

Table 2. The sixty two formulations obtained from different polymer combinations.

	Polymeric Composition (mg)																								
F	P6	PL	PE	PA	CG	EC	PV	XG	GL	ML	HE	HP	BW	ES	ER	MA	MB	MC	MD	ME	MF	MG	MH	MI	WT
1	150	150	100	200	200	-	-	-	-	-	-	-	-	-	-	-	-	-	-	-	-	-	-	-	800
2	100	150	150	200	100	-	-	-	-	-	-	-	-	-	-	-	-	-	-	-	-	-	-	-	800
3	100	100	200	250	150	-	-	-	-	-	-	-	-	-	-	-	-	-	-	-	-	-	-	-	800
4	130	155	170	205	140	-	-	-	-	-	-	-	-	-	-	-	-	-	-	-	-	-	-	-	800
5	120	180	160	210	130	-	-	-	-	-	-	-	-	-	-	-	-	-	-	-	-	-	-	-	800
6	200	150	150	200	100	-	-	-	-	-	-	-	-	-	-	-	-	-	-	-	-	-	-	-	800
7	105	155	105	205	195	-	-	-	-	-	-	-	-	-	-	-	-	-	-	-	-	-	-	-	800
8	110	165	120	230	175	-	-	-	-	-	-	-	-	-	-	-	-	-	-	-	-	-	-	-	800
9	140	160	110	240	150	-	-	-	-	-	-	-	-	-	-	-	-	-	-	-	-	-	-	-	800
10	230	120	100	110	240	-	-	-	-	-	-	-	-	-	-	-	-	-	-	-	-	-	-	-	800
11	210	105	130	205	250	-	-	-	-	-	-	-	-	-	-	-	-	-	-	-	-	-	-	-	800
12	205	150	145	200	100	-	-	-	-	-	-	-	-	-	-	-	-	-	-	-	-	-	-	-	800
13	150	300	150	200	-	-	-	-	-	-	-	-	-	-	-	-	-	-	-	-	-	-	-	-	800
14	250	200	150	200	-	-	-	-	-	-	-	-	-	-	-	-	-	-	-	-	-	-	-	-	800
15	50	300	125	125	-	200	-	-	-	-	-	-	-	-	-	-	-	-	-	-	-	-	-	-	800
16	50	200	125	125	-	300	-	-	-	-	-	-	-	-	-	-	-	-	-	-	-	-	-	-	800
17	50	150	125	125	-	350	-	-	-	-	-	-	-	-	-	-	-	-	-	-	-	-	-	-	800
18	50	100	125	125	-	400	-	-	-	-	-	-	-	-	-	-	-	-	-	-	-	-	-	-	800
19	150	250	-	125	-	275	-	-	-	-	-	-	-	-	-	-	-	-	-	-	-	-	-	-	800
20	150	225	-	175	-	250	-	-	-	-	-	-	-	-	-	-	-	-	-	-	-	-	-	-	800
21	150	200	-	225	-	225	-	-	-	-	-	-	-	-	-	-	-	-	-	-	-	-	-	-	800
22	160	250	-	190	-	200	-	-	-	-	-	-	-	-	-	-	-	-	-	-	-	-	-	-	800
23	170	250	-	205	-	175	-	-	-	-	-	-	-	-	-	-	-	-	-	-	-	-	-	-	800
24	180	250	-	220	-	150	-	-	-	-	-	-	-	-	-	-	-	-	-	-	-	-	-	-	800
25	190	250	-	235	-	125	-	-	-	-	-	-	-	-	-	-	-	-	-	-	-	-	-	-	800
26	195	250	-	225	-	100	-	-	-	-	-	-	-	-	-	-	-	-	-	-	-	-	-	-	800
27	200	250	-	25	-	300	25	-	-	-	-	-	-	-	-	-	-	-	-	-	-	-	-	-	800
28	175	250	-	25	-	300	50	-	-	-	-	-	-	-	-	-	-	-	-	-	-	-	-	-	800
29	150	250	-	25	-	300	75	-	-	-	-	-	-	-	-	-	-	-	-	-	-	-	-	-	800
30	125	250	-	25	-	300	100	-	-	-	-	-	-	-	-	-	-	-	-	-	-	-	-	-	800
31	100	250	-	25	-	300	125	-	-	-	-	-	-	-	-	-	-	-	-	-	-	-	-	-	800
32	220	275	-	25	-	250	25	5	-	-	-	-	-	-	-	-	-	-	-	-	-	-	-	-	800
33	215	275	-	25	-	250	25	10	-	-	-	-	-	-	-	-	-	-	-	-	-	-	-	-	800
34	210	275	-	25	-	250	25	15	-	-	-	-	-	-	-	-	-	-	-	-	-	-	-	-	800
35	205	275	-	25	-	250	25	20	-	-	-	-	-	-	-	-	-	-	-	-	-	-	-	-	800
36	200	275	-	25	-	250	25	25	-	-	-	-	-	-	-	-	-	-	-	-	-	-	-	-	800
37	195	275	-	25	-	250	25	30	-	-	-	-	-	-	-	-	-	-	-	-	-	-	-	-	800
38	190	275	-	25	-	250	25	35	-	-	-	-	-	-	-	-	-	-	-	-	-	-	-	-	800
39	185	275	-	25	-	250	25	40	-	-	-	-	-	-	-	-	-	-	-	-	-	-	-	-	800
40	180	275	-	25	-	250	25	45	-	-	-	-	-	-	-	-	-	-	-	-	-	-	-	-	800
41	175	275	-	25	-	250	25	50	-	-	-	-	-	-	-	-	-	-	-	-	-	-	-	-	800
42	195	300	-	25	-	250	25	-	5	-	-	-	-	-	-	-	-	-	-	-	-	-	-	-	800
43	185	300	-	25	-	250	25	-	15	-	-	-	-	-	-	-	-	-	-	-	-	-	-	-	800
44	175	300	-	25	-	250	25	-	25	-	-	-	-	-	-	-	-	-	-	-	-	-	-	-	800
45	165	300	-	25	-	250	25	-	35	-	-	-	-	-	-	-	-	-	-	-	-	-	-	-	800
46	155	300	-	25	-	250	25	-	45	-	-	-	-	-	-	-	-	-	-	-	-	-	-	-	800
47	175	300	-	25	-	250	25	-	-	25	-	-	-	-	-	-	-	-	-	-	-	-	-	-	800
48	175	300	-	25	-	250	25	-	-	-	25	-	-	-	-	-	-	-	-	-	-	-	-	-	800
49	175	300	-	25	-	250	25	-	-	-	-	25	-	-	-	-	-	-	-	-	-	-	-	-	800
50	175	300	-	25	-	250	25	-	-	-	-	-	25	-	-	-	-	-	-	-	-	-	-	-	800
51	175	300	-	25	-	250	25	-	-	-	-	-	-	25	-	-	-	-	-	-	-	-	-	-	800
52	175	300	-	25	-	250	25	-	-	-	-	-	-	-	25	-	-	-	-	-	-	-	-	-	800
53	150	400	-	25	-	150	25	-	-	-	-	-	-	-	-	50	-	-	-	-	-	-	-	-	800
54	150	400	-	25	-	150	25	-	-	-	-	-	-	-	-	-	50	-	-	-	-	-	-	-	800
55	150	400	-	25	-	150	25	-	-	-	-	-	-	-	-	-	-	50	-	-	-	-	-	-	800
56	150	400	-	25	-	150	25	-	-	-	-	-	-	-	-	-	-	-	50	-	-	-	-	-	800

Continued

Table 2. Continued.

	Polymeric Composition (mg)																							
F	P6	PL	PE	PA	CG	EC	PV	XG	GL	ML	HE	HP	BW	ES	ER	MA	MB	MC	MD	ME	MF	MG	MH	MI	WT
57	150	400	-	25	-	150	25	-	-	-	-	-	-	-	-	-	-	-	-	50	-	-	-	-	800
58	150	400	-	25	-	150	25	-	-	-	-	-	-	-	-	-	-	-	-	-	50	-	-	-	800
59	75	400	-	25	-	200	25	-	-	-	-	-	-	-	-	-	-	-	-	-	-	75	-	-	800
60	75	400	-	25	-	200	25	-	-	-	-	-	-	-	-	-	-	-	-	-	-	-	75	-	800
61	75	400	-	25	-	200	25	-	-	-	-	-	-	-	-	-	-	-	-	-	-	-	-	75	800
62	150	400	-	25	-	200	25	-	-	-	-	-	-	-	-	-	-	-	-	-	-	-	-	-	800

F: Formulation number; **P6:** Modified polyamide 6,10; **PL:** Poly(lactic-co-glycolic acid); **PE:** Polyethylene oxide **PA:** Polyacrylic acid; **CG:** Carrageenan; **EC:** Ethycellulose; **PV:** Polyvinylalcohol; **XG:** Xanthan gum; **GL:** gelatin; **ML:** Methylcellulose; **HE:** Hydroxyethylcellulose; **HP:** Hydroxypropylcellulose; **BW:** beeswax; **ES:** Eudragit S100; **ER:** Eudragit RS 100; **MA, MB, MC, MD, ME, MF:**Mixture of two polymers among gelatin, beeswax, xanthan gum and Eudragit S 100 25mg each; **MG, MH, MI:** [For the Mixture of three polymers among gelatin, beeswax, xanthan gum and Eudragit S 100 25mg [For the mixture of two polymers, MA was GL+ES; MB: GL+BW; MC: ES+BW; MD: ES+XG; ME: BW+XG and MF: GL+XG while for the mixture of three polymers, MG was GL+ES+BW; MH: GL+BW+XG and MI: ES+BW+XG].

Hainburg, Germany) while friability was conducted on a Friabilator (Erweka D-63150, Heusenstamm, Germany) at 25 rpm for 4 min with 1% set as the upper limit of acceptability. The weight of each device was determined using an analytical digital balance (Mettler, Model AE 240, Griefensee, Switzerland) with readings recorded to 2 decimal places.

For the mixture of two polymers, MA was GL+ES; MB: GL+BW; MC: ES+BW; MD: ES+XG; ME: BW+XG and MF: GL+XG while for the mixture of three polymers, MG was GL+ES+BW; MH: GL+BW+XG and MI: ES+BW+XG.

Statistical design and optimization approach as a pivot for the development of lead intravaginal bioadhesive polymeric devices

An Extreme Vertices Mixture Design experimental formulation template was generated employing Minitab® V15 (Minitab® Inc., State College, PA) statistical software to produce various caplet formulations comprising 11 polymer combinations (Table 3). Each formulation had an equivalent mass of 800 mg. Formulation response optimization was performed using an inherent D-optimal technique by combining mixture components and processing factors to converge to pre-optimal settings prior to achieving a global optimized solution with the desirable polymeric proportions for the AS-PAA and APE-PAA caplets that were subsequently prepared and further tested. The various polymers were weighed in triplicate and subsequently blended with magnesium stearate (0.5% w/w) using a cube blender (Erweka Apparatebau). The blends were then granulated with 96.5% ethanol and dried at room temperature (21°C) over 24 h prior to compression into caplets devices using a Carver Press (Carver Inc. Hydraulic Laboratory Press) at a force of 5 tons.

Equilibrium swelling studies conducted on the preliminary formulations as a critical indicator of the formulation's matrix stability

A polymer combination selected as a working formulation onto which the OVAT approach was applied in an attempt to find lead polymers for formulating IBPD was: $_{m}$PA 6,10 (50 mg), PLGA (300 mg), PEO (125 mg), PAA (125 mg) and CG (200 mg). A series of swelling tests were conducted on various sets of the formulations shown in Table 2 to investigate which device would have the optimal swelling at both human and pig vaginal fluids pH (i.e. ~4.5) and human/pig seminal fluids pH (i.e. ~7.4), by employing the OVAT approach. Due to the physiological similarity between the human and pig[53–56], simulated human vaginal and seminal fluids[57,58] prepared as indicated in Table 4, were employed for the tests. Each of the tested devices was weighed, immersed into both simulated fluids and then placed in an orbital shaking incubator (MRC Laboratory Instruments Ltd., Hahistadrut, Holon, Israel), maintained at 20 rpm and a temperature of 37°C for 24 h. After 24 h each device was removed from the orbital shaking incubator, gently blotted on a filter paper and then re-weighed. The swelling behavior was determined in terms of the equilibrium swelling ratio (ESR) which was calculated using Equation 1. The ESR (after 24 h) which was the critical indicator of the formulation's matrix stability (i.e. the degree of matrix robustness), was in this case used as a screening parameter for each formulation.

$$ESR = \frac{W_t - W_0}{W_0} \quad (1)$$

Table 3. Extreme vertices mixture design formulation template for caplet preparation.

Formulation Number	PA 6,10 (mg)	PLGA (mg)	PEO (mg)	PAA[a/b] (mg)	CG (mg)
1	150	50	200	200	200
2	100	50	250	200	200
3	100	50	200	250	200
4	130	55	205	205	205
5	105	80	205	205	205
6	100	100	200	200	200
7	105	55	205	205	230
8	105	55	205	230	205
9	110	60	210	210	210
10	100	50	200	200	250
11	105	55	230	205	205

[a]allyl sucrose-crosslinked PAA.
[b]allyl penta erythritol-crosslinked PAA.

Table 4. Constituents used to prepare the simulated human vaginal and seminal fluids

SHVF[1]		SHSF[2]	
Component	Quantity (g/L)	Component	Quantity (g/L)
NaCl	3.510	$NaH_2PO4{\cdot}H_2O$	16.974
KOH	1.400	Na_2HPO_4	17.466
$Ca(OH)_2$	0.222	$Na_3C_3H_5O(CO_2)_3$	8.130
Bovine serum albumin	0.018	KCl	0.908
Lactic acid	2.000	KOH	0.881
Acetic acid	1.000	$CaCl_2$	1.010
Glycerol	0.160	$MgCl_2$	0.920
Urea	0.400	$ZnCl_2$	0.344
Glucose	5.000	Glucose	1.020
		Fructose	2.720
		Urea	0.450
		Lactic acid	0.620
		Bovine serum albumin	50.400

[1]Simulated human vaginal fluid according to Owen and Katz[58].
[2]Simulated human seminal fluid according to Owen and Katz[57].

Table 5. Formulations without carrageenan.

	Polymeric composition (mg)			
F #	$_m$PA 6,10	PLGA	PAA	PEO
1	50.0	400.0	250.0	100
2	100.0	350.0	250.0	100
3	200.0	250.0	250.0	100
4	250.0	200.0	250.0	100
5	300.0	150.0	250.0	100
6	350	100.0	250.0	100

where ESR is the equilibrium swelling ratio, W_o is the initial weight of the device and W_t is the weight of the device after 24 h.

Effect of changing the formulation components of the IBPD on the equilibrium swelling ratio

The formulations components of the IBPD were changed sequentially (changes highlighted in grey color in the respective Tables) to see the effect on equilibrium swelling ratio.

Effect of the elimination of carrageenan Carrageenan is a highly hydrophilic compound which is substantially water-soluble with the capacity to transform into a gel that presents with a high degree of swelling in an alkaline pH[59]. It was thus eliminated to see the effect in terms of the composite swelling of the devices. After elimination of the carrageenan an adjustment of the quantities of the remaining polymers was undertaken to maintain a constant weight of 800 mg (Table 5).

Effect of the addition of ethylcellulose Due to its hydrophobic nature and high compressibility, EC was employed to replace CG. The quantities of PAA and PEO were substantially reduced as they enhanced matrix swelling, due to their high degree of hydrophilicity. The quantities of EC employed ranged from 240 to 460 mg as shown in Table 6.

Table 6. Formulations in which carrageenan was substituted with ethylcellulose.

	Polymeric composition (mg)				
F #	$_m$PA 6,10	PLGA	PEO	PAA	EC
1	90.0	340.0	65	65.0	240.0
2	90.0	240.0	65	65.0	340.0
3	90.0	190.0	65	65.0	390.0
4	90.0	140.0	65	65.0	440.0
5	90.0	130.0	65	65.0	450.0
6	90.0	120.0	65	65.0	460.0

Table 7. Formulations without polyethylene oxide.

	Polymeric composition (mg)			
F #	$_m$PA 6,10	PLGA	PAA	EC
1	100	300.0	75.0	325
2	100	300.0	100	300
3	100	300.0	150	250
4	100	300.0	200.0	200
5	100	300.0	250.0	150
6	100	300.0	300.0	100

Table 8. Formulations containing polyvinyl alcohol.

	Polymeric composition (mg)				
F#	$_m$PA 6,10	PLGA	EC	PAA	PVA
1	200.0	250.0	300.0	25.0	25.0
2	175.0	250.0	300.0	25.0	50.0
3	150.0	250.0	300.0	25.0	75.0
4	125.0	250.0	300.0	25.0	100.0
5	100.0	250.0	300.0	25.0	125.0
6	75.0	250.0	300.0	25.0	150.0

Effect of the elimination of polyethylene oxide PEO is a hydrophilic polymer with a high tendency to undergoing swelling[60]. PEO as a bioadhesive and a rate-controlling polymer was removed to reduce the number of hydrophilic polymers so as to reduce the extent of swelling of the devices. However, PAA remained included throughout all formulations due to its substantial bioadhesive-imparting tendency (Table 7).

Effect of the addition of polyvinyl alcohol PVA has high tensile strength and flexibility, as well as adhesive and high oxygen barrier properties[61–63]. It is also an atactic material but exhibits crystallinity as the hydroxyl groups are small enough to fit into the lattice without disrupting it. It was therefore incorporated into the formulation to enhance the control of drug release as well as the bioadhesivity of the devices. Quantities ranging from 25 to 150 mg were employed in formulations to produce a total weight of 800 mg/device while keeping the quantities of PLGA, EC and PAA constant (Table 8).

Effect of the addition of polyvinyl povidone PVP is a water-soluble material with a Newtonian-type viscosity. When

dry it is a light flaky powder, capable of readily absorbing up to 40% of its weight in atmospheric water. In solution, it has excellent wetting properties and readily forms films which make it a good coating agent. It was therefore added to the formulations ranging from 25 to 150 mg with the intention of fostering the bioadhesivity of the devices. The quantities of PLGA, EC and PAA were kept constant as shown in Table 9.

Effect of the addition of xanthan gum XG is a water-soluble polysaccharide produced by *Xanthomonas campestris*. It forms a single or double-stranded helix in dilute solution that transforms into molecular assemblages which show liquid crystallinity in the presence of water[64,65]. XG can form hydrogels upon annealing its solution in the sol state and then cooling[66,67]. XG was therefore added to the formulations due to its gel-forming and viscosity-enhancing properties in an attempt to facilitate adhesion of the device to the vaginal epithelium. The quantities added ranged from 5 to 50 mg. The quantities of PLGA, EC, PAA and PVA were kept constant (Table 10).

Effect of the addition of guar gum GG is a polysaccharide comprising galactose and mannose. In water it is non-ionic and hydrocolloidal and remains stable in solution over a pH range of 5–7. Guar gum presents with high low-shear viscosity but is strongly shear-thinning. It is very thixotropic above 1%$^{w}/_{v}$ with a low degree of thixotropy below a concentration of 0.3%$^{w}/_{v}$[68]. It shows viscosity synergy with xanthan gum. Guar gum has almost eight times the water-thickening potency of other thickening agents such as starch, and therefore can be used in the preparation of various multi-phase formulations[69]. It was therefore added to the current formulations so as to enhance the bioadhesivity. The quantities added ranged from 5 to 50 mg (Table 11).

Table 9. Formulations containing polyvinyl povidone.

	Polymeric composition (mg)				
F #	$_{m}$PA 6,10	PLGA	EC	PAA	PVP
1	200.0	250.0	300.0	25.0	25.0
2	175.0	250.0	300.0	25.0	50.0
3	150.0	250.0	300.0	25.0	75.0
4	125.0	250.0	300.0	25.0	100.0
5	100.0	250.0	300.0	25.0	125.0
6	50.0	250.0	300.0	25.0	150.0

Table 10. Formulations containing xanthan gum.

	Polymeric composition (mg)					
F #	$_{m}$PA 6,10	PLGA	EC	PAA	PVA	XG
1	220.0	275.0	250.0	25.0	25.0	5.0
2	210.0	275.0	250.0	25.0	25.0	15.0
3	200.0	275.0	250.0	25.0	25.0	25.0
4	190.0	275.0	250.0	25.0	25.0	35.0
5	180.0	275.0	250.0	25.0	25.0	45.0
6	175.0	275.0	250.0	25.0	25.0	50.0

Effect of the addition of gelatin GL is a translucent, brittle, solid substance derived from the collagen obtained from skin and bones of animals. It forms a solution of high viscosity in water, which sets to a gel on cooling. Gelatin solutions present with viscoelastic flow and streaming birefringence[70]. It qualifies as a binder, and therefore was used to substitute xanthan gum in an attempt to improve the bioadhesivity of the devices. The quantities added ranged from 5 to 50 mg while the quantities of the other polymers remained constant (Table 12).

Effect of the addition of beeswax Beeswax is comprised of a mixture of many organic compounds, including hydrocarbons, wax esters, and fatty acids. It has emollient, soothing and softening properties. Furthermore, it is very stable over prolonged periods. It is resistant to hydrolysis and natural oxidization and is completely insoluble in water. Thus, beeswax was added to the formulations ranging from 5 to 50 mg (Table 13) so as to increase the matrix stability of the devices.

Effect of the addition of tragacanth Tragacanth is a translucent and horny fracture short material. It swells in water forming smooth nearly uniform stiff opalescent mucilage that is free of cellular fragments. It imparts great viscidity to water, a property that renders it useful for the suspension

Table 11. Formulations containing guar gum.

	Polymeric composition (mg)					
F #	$_{m}$PA 6,10	PLGA	EC	PAA	PVA	GG
1	220.0	275.0	250.0	25.0	25.0	5.0
2	210.0	275.0	250.0	25.0	25.0	15.0
3	200.0	275.0	250.0	25.0	25.0	25.0
4	190.0	275.0	250.0	25.0	25.0	35.0
5	180.0	275.0	250.0	25.0	25.0	45.0
6	175.0	275.0	250.0	25.0	25.0	50.0

Table 12. Formulations in which xanthan gum was substituted with gelatin.

	Polymeric composition (mg)					
F #	$_{m}$PA 6,10	PLGA	EC	PAA	PVA	GL
1	195.0	300.0	250.0	25.0	25.0	5
2	185.0	300.0	250.0	25.0	25.0	15
3	175.0	300.0	250.0	25.0	25.0	25
4	165.0	300.0	250.0	25.0	25.0	35
5	155.0	300.0	250.0	25.0	25.0	45
6	150.0	300.0	250.0	25.0	25.0	50

Table 13. Formulations in which gelatin was substituted with beeswax.

	Polymeric composition (mg)					
F #	$_{m}$PA 6,10	PLGA	EC	PAA	PVA	BW
1	195.0	300.0	250.0	25.0	25.0	5
2	185.0	300.0	250.0	25.0	25.0	15
3	175.0	300.0	250.0	25.0	25.0	25
4	165.0	300.0	250.0	25.0	25.0	35
5	155.0	300.0	250.0	25.0	25.0	45
6	150.0	300.0	250.0	25.0	25.0	50

of heavy insoluble powders. Pharmaceutically, it is has good applications particularly in imparting consistence to troches and emulsions. It was added to the formulations for its effect on the matrix stability. The quantities added ranged from 5 to 50 mg (Table 14).

Effect of the addition of methylcellulose, hydroxyethylcellulose, hydroxyl-propylcellulose, hydroxypropylmethylcellulose, Eudragit® S100 and Eudragit® RS100 as substitutes for gelatin MC, HEC, HPC and HPMC are cellulose ethers that differ in their type and degree of substitution. These polymers are hydrophilic in nature with pharmaceutical attributable properties that favor their use in the preparation of controlled release formulations. They are also used as bulking agents in the tabletting process. When exposed to aqueous media, they swell forming a gel layer around the tablet core[71]. Chain dissolution may take place at the gel surface depending on the type of cellulose ester. These polymers were added to the formulations to investigate their effect on the equilibrium swelling ratio of the devices with the intention of finally employing them to control drug release. ED-S100 and ED-RS100 are poly(ethyl acrylate, methyl-methacrylate, and chlorotrimethyl-ammoniumethylmethacrilate) co-polymers. They are insoluble at physiological pH but undergo swelling in water[72]. ED-S100 and ED-RS100 are commonly employed for the enteric coating of tablets and in the preparation of controlled release formulations. Both are good materials for the dispersion of drugs and have been used successfully to obtain appropriate controlled release matrix formulations[73–75]. They were therefore added to the formulations for the purpose of modulating the release kinetics. The quantity of each polymer added to the formulations was 25 mg. The quantities of the other polymers were kept constant (Table 15).

Table 14. Formulations containing tragacanth.

	Polymeric composition (mg)					
F #	$_m$PA 6,10	PLGA	EC	PAA	PVA	TG
1	195.0	300.0	250.0	25.0	25.0	5
2	185.0	300.0	250.0	25.0	25.0	15
3	175.0	300.0	250.0	25.0	25.0	25
4	165.0	300.0	250.0	25.0	25.0	35
5	155.0	300.0	250.0	25.0	25.0	45
6	150.0	300.0	250.0	25.0	25.0	50

Table 15. Formulations containing methylcellulose, hydroxyethylcellulose, hydroxyl-propylcellulose, hydroxypropylmethylcellulose, Eudragit® S100 and Eudragit® RS100.

	Polymeric composition (mg)					
F #	$_m$PA 6,10	PLGA	EC	PAA	PVA	Additional polymer
1	175.0	250.0	300.0	25.0	25.0	25 (MC)
2	175.0	250.0	300.0	25.0	25.0	25 (HEC)
3	175.0	250.0	300.0	25.0	25.0	25 (HPC)
4	175.0	250.0	300.0	25.0	25.0	25 (HPMC)
5	175.0	250.0	300.0	25.0	25.0	25(ED-S100)
6	175.0	250.0	300.0	25.0	25.0	25 (ED-RS100)

Effect of the addition of a binary polymer combination to the formulation Combinations of 2 polymers in equal quantities of 25 mg each (1:1), from among gelatin, beeswax, xanthan gum and ED-S100 were added to the formulations to investigate their effect on the matrix stability. The quantities of the other polymers were kept constant (Table 16).

Effect of the addition of a tertiary polymer combination to the formulation Combinations of 3 polymers in equal quantities of 25 mg each (1:1:1), from among gelatin, beeswax, xanthan gum and ED-S100 were added to the formulations to investigate the effect on the matrix stability of the devices. The quantities of the other polymers were kept constant (Table 17).

X-imaging to explicate the swelling and erosion dynamics of the intravaginal bioadhesive polymeric device in the pig model Three Large White pigs each weighing 35 kg were anesthetized with midazolam (0.3 mg/kg I.M.) and ketamine (11 mg/kg I.M.). Two percent isoflurane in 100% oxygen was administered via a face mask to maintain anesthesia. The IBPD was then deeply inserted into the posterior fornix of the vagina of each pig with the aid of an applicator and a speculum. To detect the swelling and erosion dynamics of the IBPD, pigs were X-rayed (Siemens AG, Medical Engineering Group, Erlangen, Germany) for a total number of 28 days as follows; directly after device insertion and thereafter three times weekly for 2 weeks, then twice weekly for a further 2 weeks.

Thermal analysis on the constituent polymers Drug-polymer compatibility studies were carried out by performing thermal analysis on the constituent polymers (i.e. $_m$PA 6,10, PLGA, PAA, PVA, and EC) as well as the IBPD using Temperature Modulated Differential Scanning Calorimetry (TMDSC) (Mettler Toledo, DSC1,

Table 16. Formulations with a binary polymer combination among gelatin, beeswax, xanthan gum and Eudragit® S100

	Polymeric composition (mg)					
F #	$_m$PA 6,10	PLGA	EC	PAA	PVA	Combination of 2 polymers
1	150.0	400.0	150.0	25.0	25.0	50 (GL+ED-S100)
2	150.0	400.0	150.0	25.0	25.0	50 (GL+BWX)
3	150.0	400.0	150.0	25.0	25.0	50 (ED-S100+BWX)
4	150.0	400.0	150.0	25.0	25.0	50 (ED-S100+XG)
5	150.0	400.0	150.0	25.0	25.0	50 (BWX+XG)
6	150.0	400.0	150.0	25.0	25.0	50 (GL+XG)

Table 17. Formulations with a tertiary polymer combination among gelatin, beeswax, xanthan gum and Eudragit® S100

	Polymeric composition (mg)					
F #	$_m$PA 6,10	PLGA	EC	PAA	PVA	Combination of 3 polymers
1	75.0	400.0	200.0	25.0	25.0	75(GL+ED-S100+BWX)
2	75.0	400.0	200.0	25.0	25.0	75 (GL+BWX+XG)
3	75.0	400.0	200.0	25.0	25.0	75 (ED-S100+BWX+XG)

Table 18. Temperature modulated DSC settings employed for thermal analysis of the intravaginal bioadhesive polymeric device

Segment type	Parameter setting
SINE PHASE[a]	
Start	–35°C
Heating rate	1°C/min
Amplitude	0.8°C
Period	0.8°C
LOOP PHASE[b]	
To segment	1
Increment	0.8°C
End	230°C
Count	436

[a]Sinusoidal oscillations.
[b]Oscillation period.

STARe System, Schwerzenback, Switzerland) in order to assess the individual thermal behavioral transitions. The parameter settings employed for thermal analysis of the intravaginal bioadhesive polymeric device are depicted in Table 18. The thermal events were explicated in terms of the glass transition (T_g) measured as the reversible heat flow (ΔH) due to changes in the magnitude of the Cp-complex values (Δ_{Cp}), melting (Tm), and crystallization (T_c) temperature peaks which are consequences of irreversible and reversible ΔH values corresponding to the total heat flow. The temperature calibration was accomplished with the melting transition of indium. The transitions of the individual polymers and their physical mixtures were compared with the transition of the composite IBPD matrix. Samples were weighed (5 mg) on perforated 40 μL aluminum pans, crimped, and then ramped from –35 to 230°C on TMDSC under a nitrogen atmosphere (Afrox, Germiston, Gauteng, South Africa) in order to diminish oxidation at a rate of 1°C/min.

In vitro drug release analysis of AZT from the intravaginal bioadhesive polymeric device An IBPD was immersed in a 100 mL[76] simulated human vaginal fluid (SHVF) (pH 4.5; 37°C[58]) (Table 4) using a sealable glass vessel (150 mL) and placed in an orbital shaking incubator (LM-530-2, MRC Laboratory Instruments Ltd.) maintained at 20 rpm and a temperature of 37°C. For the determination of AZT concentration, 3 mL samples were withdrawn at predetermined time intervals over a period of 30 days and subjected to ultra performance liquid chromatography analysis. An equivalent volume of drug-free SHVF was replaced into the release medium to maintain sink conditions. The analysis was conducted in triplicate. A correction factor was appropriately applied in all cases where dilution of samples was required.

Ex vivo bioadhesivity testing of the intravaginal bioadhesive polymeric device >Excision of vaginal tissue from the pig model. A large white female pig (84 kg) was euthanized with 40 mL of sodium pentobarbitone (200 mg/mL) administered intravenously. The pelvic canal of the pig was opened by dissecting through the symphysis pubis and then exposing the intra-abdominal vaginal tract (the vestibulum). The external vaginal tract was carefully dissected from the surrounding tissues before removing the vaginal tissue. An incision was made through the vaginal canal to expose the inner lining of the tissue, which was then placed in an airtight specimen jar and immediately subjected to bioadhesivity testing.

Textural profiling analysis to determine the bioadhesivity of the intravaginal bioadhesive polymeric device. Bioadhesivity of the IBPD was determined using a previous textural profile analysis method developed by Ndesendo and co-workers[77]. Briefly, the freshly excised pig vaginal tissue was secured on the textural probe and the IBPD was fixated onto the heated textural platen after exposure to SHVF (pH 4.5, 37°C) for 30 min. Testing was then conducted by measuring the maximum force (N) required to detach the vaginal tissue from the fixated device. This was determined by measuring the peak adhesive force (PAF) or the work of adhesion that was computed as the area under the curve of a force–distance textural profile (AUC_{FD}). The conditions under which bioadhesivity testing was undertaken constituted a simulated clinical environment using a modified textural analysis experimental technique. A heated platen (37 ± 0.5°C) was used to maintain simulated vaginal conditions prior to fixating the IBPD and during analysis. In addition, all experimentation was performed using simulated human vaginal fluid (pH 4.5; 37°C) as the bioadhesivity test medium.

Postulated mechanism of the IBPD swelling dynamics employing chemometric modeling

Chemometric and molecular structural modeling was used to deduce the transient mechanisms of chemical interactions and inter-polymeric interfacing during swelling of the IBPD. This approach allowed us to make predictive findings based on the chemical and physical interactions underlying the swelling dynamics of the IBPD when immersed in SHVF In addition, semi-empirical quantum mechanics were employed to generate molecular interactions and computational energy paradigms of the IBPD components based on inherent interfacial phenomena underlying the mechanisms of swelling as provided by the inter-polymeric blended IBPD. Models and graphics supported on the step-wise molecular IBPD-simulated fluids, polymeric interconversion, diffusion and erosion as envisioned by the molecular behavior and stability of the gelled IBPD network were generated on ACD/I-Lab, V5.11 (Add-on) software (Advanced Chemistry Development Inc., Toronto, Canada, 2000).

Molecular mechanics simulations of the sterically constrained and geometrically optimized multi-polymeric complex, IBPD

Molecular mechanics computations, which included the model building of the energy-minimized structures of multi-polymer complexes (MPC) consisting of combinations of PLGA, $_m$PA6,10, PVA, PEO, PAA, EC or CRG such as PLGA-$_m$PA6,10 (MPC1), PLGA-$_m$PA6,10-PVA (MPC2), PLGA-$_m$PA6,10-PVA-PAA (MPC3),

PLGA-$_m$PA6,10-PVA-PEO (MPC4), PLGA-$_m$PA6,10-PVA-PEO-EC (MPC5), PLGA-$_m$PA6,10-PVA-PAA-CRG (MPC6) and PLGA-$_m$PA6,10-PVA-PAA-EC (MPC7) were conducted and disposed in different spatial conformations. The generation of the overall steric energy associated with the energy-minimized structures was performed with using the HyperChem™ 8.0.8 Molecular Modeling System (Hypercube Inc., Gainesville, FL) and ChemBio3D Ultra 11.0 (CambridgeSoft Corporation, Cambridge, UK) on a Pentium T3200 workstation. The octamer of PLGA, dimer of $_m$PA6,10 and decamers of PVA, PEO and PAA were generated from standard bond lengths and angles employing polymer builder tools using ChemBio3D Ultra in their syndiotactic stereochemistry as 3D models whereas the structures of EC and CRG (four iligosaccharide units each) were generated using sugar builder module on HyperChem 8.0.8. The individual polymer models and MPC models were initially energy-minimized using MM+ force field and the resulting structures were again energy-minimized using the Amber 3 (Assisted Model Building and Energy Refinements) force field. The conformer having the lowest energy was used to create the polymer-polymer complexes. A complex of one molecule with another was assembled by disposing them in a parallel way, and the same procedure of energy-minimization was repeated to generate the final models. Full geometry optimizations were carried out in vacuum employing the Polak–Ribiere conjugate gradient method until an RMS gradient of 0.001 kcal/mol was reached. Force field options in the AMBER (with all hydrogen atoms explicitly included) and MM+ (extended to incorporate non-bonded cut-offs and restraints) methods were the HyperChem 8.0.8 defaults. The MM simulations in solvated system were performed for cubic periodic boxes with a side length of 25.97Å containing the MPC at the centre of the cubic box and the remaining free space filled with water molecules and the same procedure of energy-minimization was repeated to generate the solvated models. Additionally, the force field options in the AMBER (with explicit solvent) were extended to incorporate cut-offs to inner and outer options with the nearest-image periodic boundary conditions. The outer cut-off was set to 12.98Ångstroms and the inner cut-off was set to 8.98Å to ensure that there were no discontinuities in the potential surface.

Results and discussion

Physical properties of $_m$PA 6,10 and in-process validation tests

The synthesized $_m$PA 6,10 product presented as a firm white crystalline spherical compact. The unrefined $_m$PA 6,10 powder was subsequently sieved through an aperture size of 1 mm in keeping with the other polymeric components of the caplet matrix to obtain a particle size ranging from 0.8 to 1.2 mm which facilitated desirable powder compression properties. The compressed caplets (Figure 3) were sufficiently strong and robust (i.e. sturdy and with high resilience) with an average

Figure 3. A digital image of the intravaginal bioadhesive polymeric devices.

Table 19. Mass, friability and longitudinal crushing force of the sixty two caplet formulations.

F#	Mass (mg)	±SD	% Friability	±SD	Longitudinal Crushing Force (N)	±SD
1	789.22	3.633	0.39	0.018	284.81	1.311
2	803.65	4.109	0.41	0.019	285.76	1.317
3	788.11	2.998	0.44	0.020	284.28	1.309
4	799.06	3.678	0.42	0.019	284.82	1.313
5	800.09	4.003	0.40	0.018	284.92	1.315
6	801.89	4.006	0.40	0.018	285.61	1.318
7	798.09	3.593	0.42	0.019	285.90	1.319

(*Continued*)

Table 19. Mass, friability and longitudinal crushing force of the sixty two caplet formulations. (*Continued*)

F#	Mass (mg)	±SD	% Friability	±SD	Longitudinal Crushing Force (N)	±SD
8	788.72	3.701	0.41	0.020	285.82	1.317
9	804.29	4.015	0.39	0.017	285.09	1.312
10	803.22	4.012	0.39	0.015	284.41	1.308
11	804.21	4.018	0.46	0.024	280.63	1.309
12	790.32	3.456	0.37	0.013	285.71	1.326
13	800.33	4.009	0.35	0.011	285.92	1.328
14	803.43	4.013	0.36	0.013	286.03	1.330
15	805.21	4.127	0.33	0.010	286.41	1.338
16	802.44	4.018	0.32	0.010	286.65	1.339
17	801.29	4.003	0.32	0.012	286.91	1.400
18	801.29	4.003	0.30	0.009	287.25	1.403
19	803.64	4.012	0.29	0.009	287.07	1.401
20	789.08	3.987	0.28	0.007	287.38	1.328
21	789.00	3.967	0.26	0.005	286.82	1.330
22	805.78	4.134	0.27	0.006	286.71	1.338
23	788.99	3.556	0.31	0.011	286.52	1.339
24	801.98	4.007	0.33	0.013	286.33	1.400
25	800.37	4.001	0.32	0.013	287.18	1.403
26	789.98	3.897	0.30	0.010	288.97	1.401
27	810.02	5.004	0.24	0.005	289.36	1.428
28	801.99	4.120	0.29	0.009	287.66	1.429
29	788.89	3.898	0.30	0.010	287.94	1.407
30	802.77	4.108	0.31	0.010	286.84	1.330
31	807.22	4.130	0.32	0.012	286.62	1.338
32	789.69	3.789	0.34	0.012	285.51	1.339
33	803.11	4.015	0.37	0.015	285.42	1.400
34	801.25	4.001	0.35	0.014	285.08	1.403
35	800.66	4.002	0.33	0.013	284.93	1.381
36	798.76	3.972	0.30	0.009	287.19	1.328
37	792.53	3.864	0.32	0.010	287.28	1.330
38	801.48	3.999	0.33	0.013	287.39	1.338
39	790.98	3.870	0.26	0.010	288.14	1.429
40	808.79	4.137	0.29	0.010	287.66	1.400
41	789.98	2.987	0.27	0.012	288.49	1.403
42	803.44	4.121	0.35	0.009	285.65	1.401
43	802.00	4.002	0.36	0.009	285.23	1.428
44	788.89	2.998	0.29	0.007	287.09	1.429
45	801.66	4.006	0.33	0.005	285.25	1.407
46	787.98	2.999	0.37	0.006	285.73	1.326
47	799.86	3.003	0.39	0.011	284.93	1.328
48	808.00	4.985	0.36	0.013	285.06	1.330
49	803.33	4.006	0.38	0.013	285.34	1.338
50	800.30	4.000	0.31	0.010	286.78	1.339
51	803.01	3.998	0.24	0.005	289.02	1.423
52	808.22	5.000	0.25	0.005	288.77	1.328
53	789.56	3.979	0.32	0.012	285.88	1.330
54	809.29	5.001	0.29	0.010	286.23	1.338
55	804.44	4.110	0.33	0.010	285.56	1.429
56	789.79	3.961	0.30	0.012	285.68	1.400
57	800.67	3.998	0.30	0.012	286.05	1.403
58	804.58	4.029	0.34	0.015	285.83	1.301
59	798.98	4.001	0.37	0.014	285.07	1.328
60	802.44	4.008	0.32	0.013	285.41	1.329
61	789.88	3.989	0.31	0.009	285.90	1.307
62	800.45	4.007	0.23	0.006	289.69	1.425

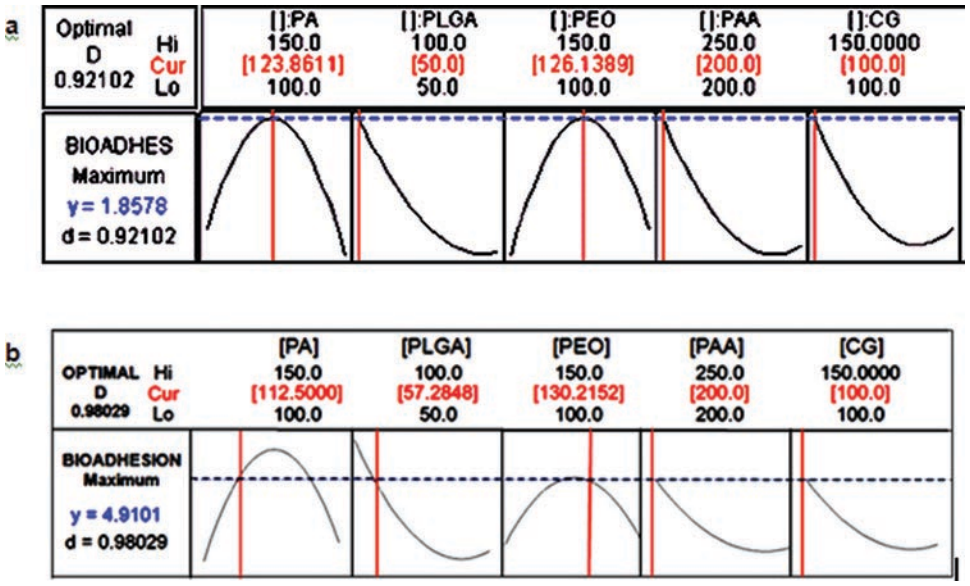

Figure 4. A typical response optimization plot for the: a) AS-PAA; and b) APE-PAA caplets.

longitudinal crushing force of 286 ± 0.03 N, a uniformity mass of 800 ± 0.48 mg and average friability of 0.31 ± 0.04% which was within the set limits (Table 19).

Response optimization of the AS-PAA and APE-PAA caplets

Response optimization of the AS-PAA and APE-PAA caplets using Minitab® V15 (Minitab® Inc.) software revealed the optimum level for each polymer (PA 6,10, PEO, PLGA, CG and PAA) within the caplets in order to provide the most optimal polymer combination as a pivot lead for developing the intravaginal bioadhesive polymeric devices (Figure 4). The desirability (D) value was 0.98 and 0.92, respectively (Figure 4) indicating the sufficient convergence of data toward an optimized global solution. APE-PAA caplets presented with higher D value (0.98) and therefore were employed throughout the study.

The influence of different polymeric composition on the equilibrium swelling ratio

The influence of carageenan, polyethylene oxide and ethylcellulose on the matrix stability

The formulations prepared with CG and PEO (F1-F12) (Table 2) presented with the highest level of matrix swelling as shown by their ESR values (0.55–0.76) (Table 20). The highest ESR was observed in F11 (ESR = 0.76; Table 20). This was most likely due to the hydrophilic nature of CG and PEO. These polymers, being highly hydrophilic, rapidly absorbed water which led to a high degree of swelling. A similar trend was apparent in F3 (ESR = 0.71) though to a lesser extent, due to relatively lower quantity of CG. The elimination of PEO and substitution of CG with EC resulted in a marked negative impact on matrix swelling in that a formulation with an ESR as low as 0.12 (F 19; Table 20) was obtained. This was due to the hydrophobic nature of EC.

Table 20. The equilibrium swelling ratios for the sixty two formulations that were subjected to screening using the OVAT approach.

F#	ESR	±SD
1	0.63	0.029
2	0.58	0.027
3	0.71	0.033
4	0.65	0.030
5	0.60	0.028
6	0.58	0.027
7	0.60	0.028
8	0.61	0.028
9	0.59	0.027
10	0.68	0.032
11	0.76	0.035
12	0.55	0.026
13	0.53	0.025
14	0.50	0.023
15	0.47	0.022
16	0.45	0.021
17	0.42	0.020
18	0.11	0.005
19	0.12	0.006
20	0.11	0.005
21	0.08	0.004
22	0.09	0.004
23	0.10	0.005
24	0.12	0.006
25	0.08	0.004
26	0.06	0.003
27	0.02	0.001
28	0.05	0.002
29	0.07	0.003
30	0.09	0.004
31	0.08	0.004
32	0.13	0.006
33	0.14	0.006

Continued

Table 20. Continued.

F#	ESR	±SD
34	0.15	0.007
35	0.16	0.007
36	0.06	0.003
37	0.08	0.004
38	0.08	0.004
39	0.04	0.002
40	0.05	0.002
41	0.04	0.002
42	0.14	0.006
43	0.16	0.007
44	0.06	0.003
45	0.13	0.006
46	0.15	0.007
47	0.53	0.025
48	0.49	0.023
49	0.56	0.026
50	0.07	0.003
51	0.02	0.001
52	0.03	0.001
53	0.12	0.006
54	0.09	0.004
55	0.14	0.006
56	0.12	0.006
57	0.11	0.005
58	0.13	0.006
59	0.15	0.007
60	0.14	0.006
61	0.12	0.006
62	0.01	0.001

The influence of guar gum, polyvinyl povidone, tragacanth and polyvinyl alcohol on matrix stability

GG produced matrix swelling to a large extent after 12 h. PVP and TG were found to induce initial swelling and subsequent erosion of the formulation after 24 h. PVA resulted in formulations with minimal matrix swelling (Table 20; F27; ESR = 0.02) and therefore was considered to have the most favorable matrix stability among the entire group.

The influence of xanthan gum, beeswax and gelatin on the matrix stability

Xanthan gum provided substantially swollen formulations which remained intact (no evidence of erosion), in addition to being highly bioadhesive. Overall, XG, BWX and GL at low quantities (25 mg each) (Table 20) resulted in formulations with minimal ESR (0.02–0.16). This may be due to the ability of XG, BWX and GL to form gel-like microstructure[78] which interspersed itself throughout.

The influence of the addition of methylcellulose, hydroxethylcellulose, hydroxypropylcellulose and hydroxylpropylmethylcellulose in the formulations, on matrix stability

The MC-containing formulations underwent initial massive swelling and thereafter erosion after 24 h (formulations completely collapsed). HEC, HPC and HPMC-containing formulations remained stable for at least 72 h. This finding may be attributed to the fact that these polymers are non-ionic and hydrophilic with water retention properties.

The influence of Eudragit® S100 and Eudragit® RS 100 on matrix stability

ED-S100 and ED-RS100 are random copolymers of methacrylic acid and ethyl acrylate, which are insoluble at acidic pH but become increasingly soluble in a neutral to weakly alkaline solution by forming salts[79,80]. Thus, the ED-S100- and ED-RS100-containing formulations presented with minimal swelling tendency (ESR = 0.02 and 0.03) in simulated vaginal fluid (pH 4.5) (Table 20; F51 and F52).

Equilibrium swelling ratios of the selected fifteen lead formulations screened through the OVAT approach

The ESRs for the selected 15 lead formulations are summarized in Table 21. Depending on the polymer combination and hydrophilic/hydrophobic proportions, all devices demonstrated a different swelling equilibrium as depicted by their ESR values (Table 21). Swelling ratio describes the amount of water that was contained within the device at equilibrium and is a function of the proportion between hydrophilicity and hydrophobicity in the device network structure. Ionization of the polymer functional groups, crosslinking density, charge density, and simulated vaginal fluid ionic strength, may have played a role as well in this regard. The higher the hydrophobicity the lower the ESR and the higher the hydrophilicity the higher the ESR. The opposite holds true in both cases. Low ESR is an indication of low swelling rate and therefore high matrix stability and vice versa[71,81,82]. Among the 15 lead formulations, F62 presented with the lowest ESR (0.011). These findings may be associated with the presence of a high quantity of PLGA (400 mg) in the formulation which prevented the influx of water into the IBPD matrix due to its high hydrophobicity. The presence of EC in the formulation at a relatively high quantity (200 mg) may have as well attributed to the obtained results since EC is also a polymer with high degree of hydrophobicity. Most certainly, minimal quantities of the hydrophilic polymers PAA and PVA coupled the superior matrix resilience of $_{m}$PA 6,10 contributed as well to the small ESR value of F62. ED-S100 and ED-RS100 are both pH-dependent polymer materials that are only soluble at pH above 6.0 (Ohmura et al., 1991). Thus, at the simulated vaginal fluid pH (4.5), these polymers were insoluble indicating that they may have played a role in preventing the entrance of water molecules to the IBPD matrix, therefore leading to the low ESR values obtained in F51 (ESR = 0.023) and F52 (ESR = 0.033), respectively (Table 21). The high tendency of GL, BWX and XG to form a non-collapsible networked-structure may have improved the veracity of the IBPD matrix and therefore the relatively low values of ESR values obtained in the formulations containing these

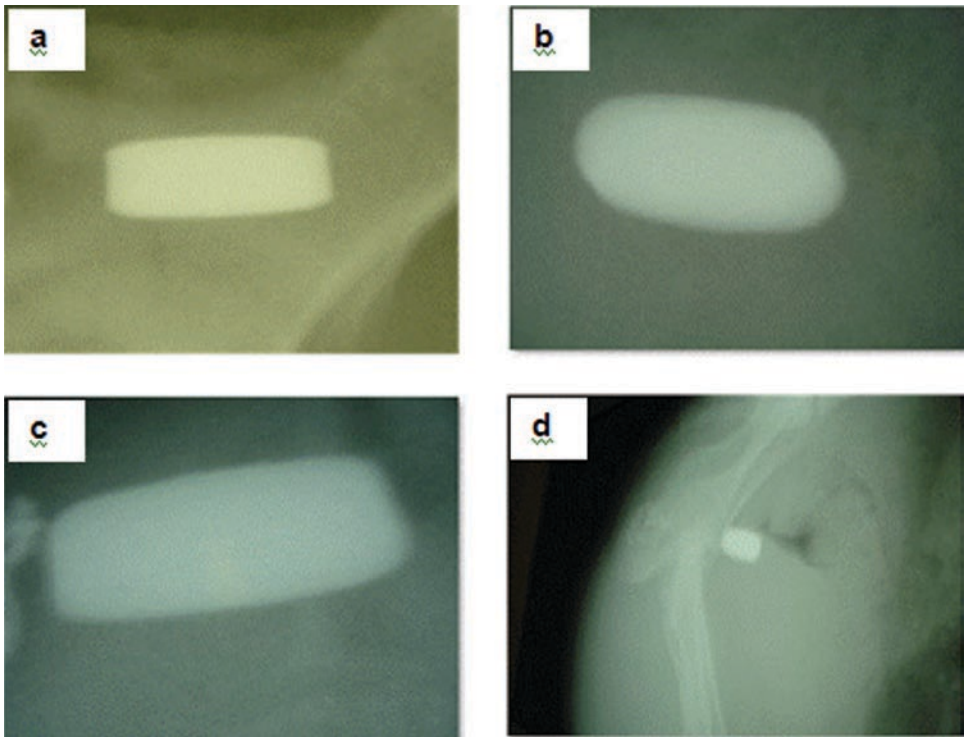

Figure 5. X-ray images swelling and erosion dynamics of the IBPD at: (a) day 1; (b) day 14; (c) day 21; and (d) day 28 after insertion into the posterior fornix of the pig vagina.

polymers (Table 21).The ESR for the best 15 formulations was in the following order F62>F27>F51>F52>F41>F39 >F28>F40>F44>F36>F29>F50>F37>F38>F31 (i.e. lowest to the highest) (Table 19). Overall, the high degree of hydrophobicity in the polymers constituting these formulations, prevented rapid penetration of water molecules into the IBPD matrix resulting in a low swelling tendency (Table 19) and therefore lower ESR values when compared to the rest of the tested formulations (Table 20).

Swelling and erosion dynamics of the IBPD in the pig model

Analysis of X-ray images (Figure 5) revealed that the IBPDs were maintained in the posterior fornix of the pig vagina for the experimental period up to 28 days. The devices underwent swelling and gradually eroded over time as shown in Figure 5a–d. On day 1, the IBPD presented with minimal change in dimensions (Figure 5a). On day 14, the IBPD had swollen a bit with an increase in size (Figure 5b). On day 21, the IBPD had swollen substantially and was still well retained within the posterior fornix of the vagina (Figure 5c), while on day 28 the IBPD presented with a high degree of erosion as substantiated by the big decrease in size (Figure 5d).

Thermal characterization of the intravaginal bioadhesive polymeric device

Thermal analysis of the IBPD revealed a T_g at 150°C, two T_c peaks at 140°C and 220°C and a T_m peak at 220°C (Figure 6). The presence of transient T_m peaks in the total TMDSC signals for the IBPD indicated that the polymers were well dispersed within the device matrix. In addition, diminutive exothermic events were observed at the corresponding T_c ranges for the constituent polymers indicating a high degree of crystallinity within the device matrix structure. The deconvolution of the total TMDSC signals for the IBPD in terms of reversing and non-reversing events reflected the average of the equivalent signals for each polymer. The T_m appeared to be predominantly reversing due to the concurrent re-crystallization and melting phenomena that offset one another. This indicated that solid–solid phase transitions may have occurred within the IBPD due to polymeric compression, and subsequently contributed to the prolongation and control of drug from the device. Thus, the thermodynamic stability of polymers/polymer blends may affect the drug release process and can therefore be used to predict the drug release behavior based on unequivocally defined thermodynamic events.

In vitro drug release analysis of AZT from the intravaginal bioadhesive polymeric device

The substantial matrix integrity imparted by the polymers used to formulate the IBPD resulted in the minimization of the rate of matrix disentanglement and consequently prolonged and controlled the release of AZT from the IBPD. AZT was released in a controlled manner from the IBPD over a period of 36 days (Figure 7). These results may be attributed to the hydrophobic nature and high compressibility of EC, PLGA and PSS, coupled with the superior matrix resilience of $_m$PA 6,10.

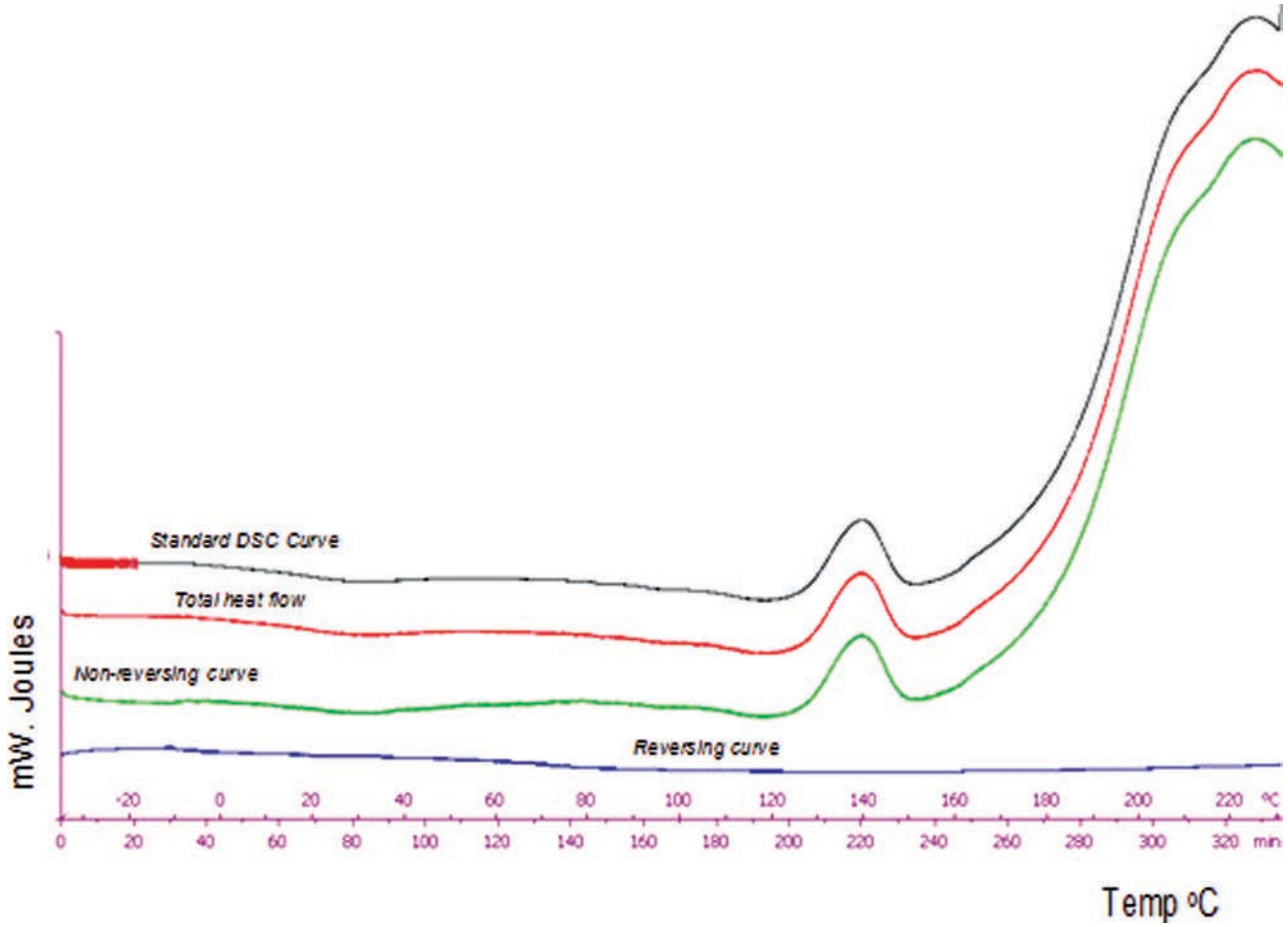

Figure 6. Temperature modulated DSC thermogram for the IBPD.

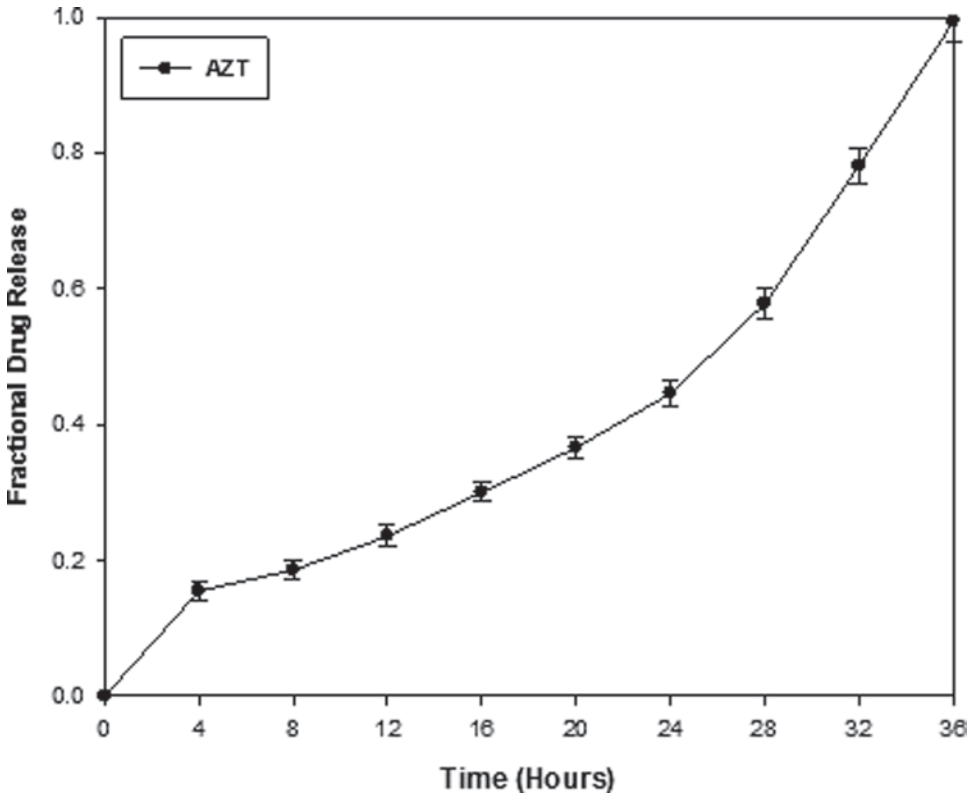

Figure 7. A drug release profile for AZT from the IBPD (pH 4.5; 37°C; $N=3$; SD < 0.18).

Ex vivo bioadhesivity analysis of the intravaginal bioadhesive polymeric device

The produced devices were strongly bioadhesive (PAF = 3.699 ± 0.0.464 N; AUC_{FD} = 0.0098 ± 0.0004 J) (Figure 8a). This indicates the superiority of PAA as a bioadhesive agent that may be attributed to its hydrophilicity, H-bonding capacity, the high molecular mass and the surface tension properties. Polyacrylic controlled the extent of interpenetration between the polymer and the vaginal mucosal/epithelial surface. The high hydrophilicity of PAA enabled the formation of strong bioadhesive bonds due to the high water content within the mucosal layer of the pig vaginal tissue. The presence of OH^- and $COOH^-$ groups in PAA may have favored the formation of H-bonds between the entangled PAA chains and the pig vaginal tissue that ultimately resulted in bioadhesion. In addition, the desirable surface tension of PAA facilitated spreading over the epithelial surface of the vaginal mucosal layer thereby enhancing bioadhesion.

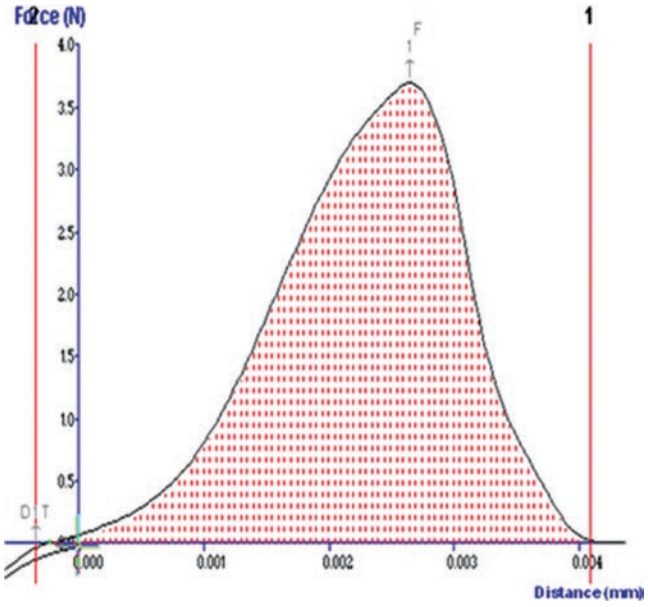

Figure 8. Typical Force-Distance textural profiles used for computing the Peak Adhesion Force (PAF) and Work of Adhesion (AUCFD) for the IBPDs on freshly excised pig vaginal tissue.

Chemometric and molecular modelling of the developmental process and swelling dynamics of intravaginal bioadhesive polymeric device

Chemometric and computational analysis revealed that polymer-polymer and polymer-drug ratios in the IBPD, as well as the components of SHVF medium contributed substantially to the swelling dynamics obtained. Figure 9 depicts a step-wise model of the IBPD developmental process as well as the swelling dynamics. Regarding the physicochemical associations of the polymers and the drugs (AZT/PSS), all components were homogenized to produce a characteristic even distribution within the IBPD matrix (Figure 9c). The hydrophilic and hydrophobic areas of certain polymeric components within the matrix and their association provided the flexible hydration sites. The hydrophilic sites were located within the outer regions of the matrix while the hydrophobic sites were confined to fewer interactive regions at the centre of the IBPD matrix (Figure 9d). AZT was confined near hydrophilic regions of the matrix while PSS consolidated the inner core as well as areas associated with other hydrophobic polymeric interactions such as PLGA and EC. The segregated hydrophilic-hydrophobic clusters within the IBPD matrix were primarily responsible for modulating the diffusion path of molecules through the matrix, which contributed substantially in enforcing the matrix stability, thereby resulting into minimal swelling.

The generation of diffusion/transport channels in the polymeric device involved inter-strand physico-chemical interactions (Figure 10a). These interactions resulted from weak and strong ionic forces as well as hydrogen bonds. Bending in a group of associated strands resulted into an interaction (Figure 10d) that generated inter-polymeric cavity depicting the horizontally located polymeric backbone as rectangular platforms joined by dotted and strong lines (Figure 10d). Figure 10f shows the associations between different polymer strands visible as squared blocks with inter-connected cavity. The biometric simulation derived through ACD/I-Lab, V5.11 (Add-on) software (Advanced Chemistry Development Inc.), that indicates the different levels of coiling that polymers undergone during inter-strand physico-chemical interactions is depicted in Figure 11. These interactions contributed significantly in controlling the diffusion

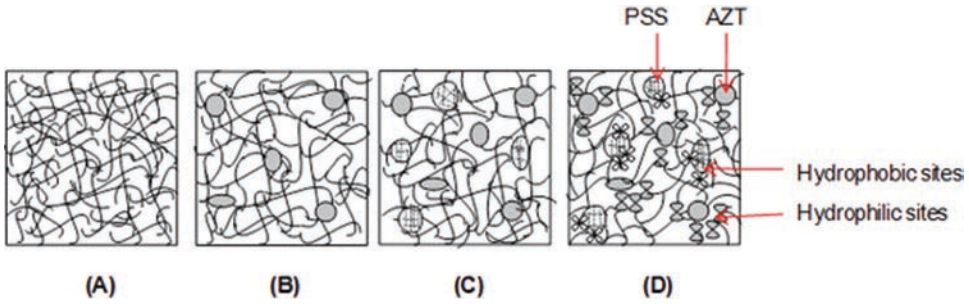

Figure 9. 1 D-Sketches representing: (A) polymer matrix, (B) water interactions giving hydrophilic pockets and swelling of the device, (C) the ingredient effects of generation of hydrophobic areas in the matrix shown with the hydrophilic pockets in the matrix, (D) the drug molecule (AZT/PSS) in association at hydrophilic and hydrophobic sites.

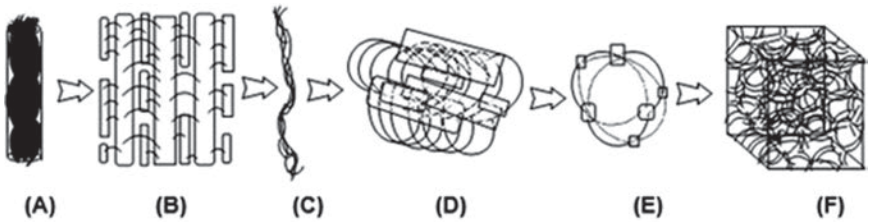

Figure 10. Generation of diffusion/transport channels in the polymeric device: (A) polymer strands, (B) inter-strand physicochemical interactions, (C) bendings in a group of associated strands, (D) the cavity, (E) associations between different polymer strands and (F) the 3D view depicting the blocked cavity.

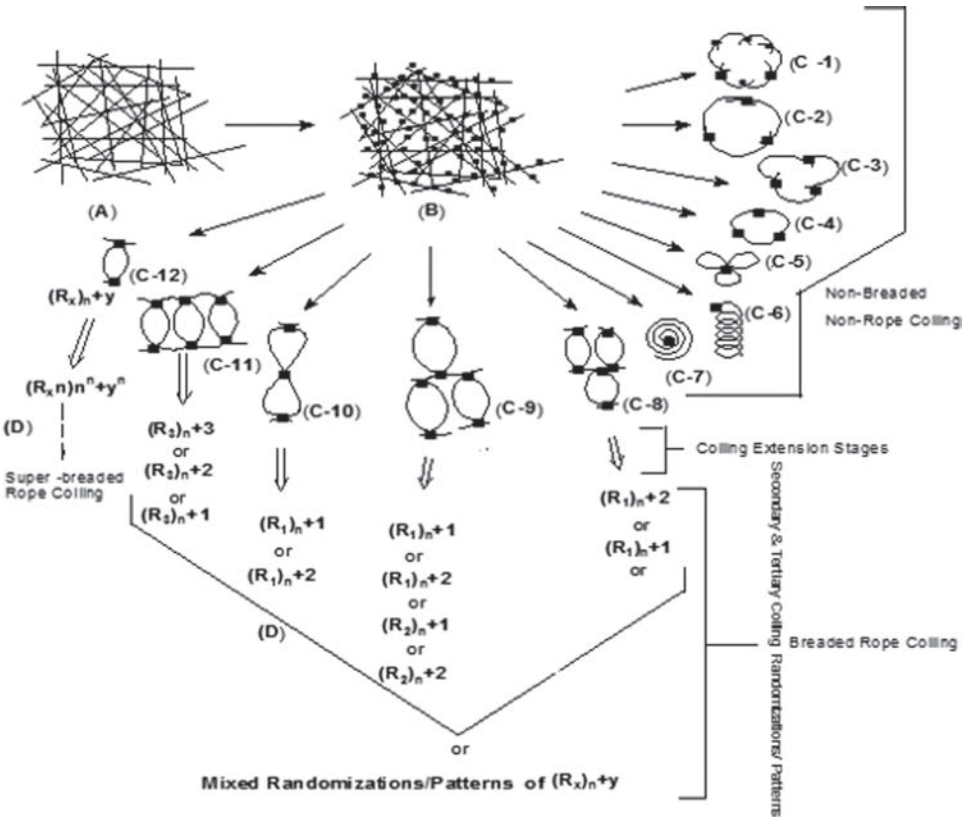

Figure 11. A computationally-derived model depicting the polymer coiling stages a) polymer strands, b) identification of molecular sites, c) initial stages of coiling, d) secondary and tertiary coiling randomizations and patterns where (C-1)-(C-7) is non-breaded non-rope coiling and (C-8)-(C-12) is breaded rope coiling. The number of coil arm may vary in (C-1)-(C-5). R1, R2 and R3 are functional groups. The lines represent polymeric strains while the blocks represent polymer strand interactions.

path that culminated into controlling the matrix swelling thereby intensifying the IBPD matrix stability.

Molecular mechanics and retro-analysis of polymer replacements

The energy minimized and equilibrated geometrical preferences of the polymer complexes derived from molecular mechanics calculations in vacuum and solvated system are shown in Figure 12a–c) and Figure 12d–f), respectively, while the respective energy transformations are displayed in Table 22. Invariant factors common to mathematical description of binding energy and substituent characteristics have been ignored. It was not possible to carry out the MM studies for all 62 formulations due to space and time constraints.

Presented here is a retro-analysis of the formulations as against the sequencing of the formulations designed in experimental section i.e. first, the optimized formulation (F62: PLGA-mPA6,10-PVA-PAA-EC) was modeled followed by replacements and additions. Therefore, experimentally screened formulation, F62, was employed as the model formulation for simulation studies and the effect of replacement of PEO with PAA and CRG with EC was elucidated as template for the addition-replacement molecular mechanics studies. The polymer assemblies were modeled employing the same OVAT approach, as in experimental section, in the form of blending simulations involving step-by-step addition of polymers, in the form of A+B (PLGA-mPA6,10), A+B+C (PLGA-mPA6,10-PVA), A+B+C+D (PLGA- mPA6,10-PVA-PAA), to finally form the IBPD penta-polymeric device (A+B+C+D+E:

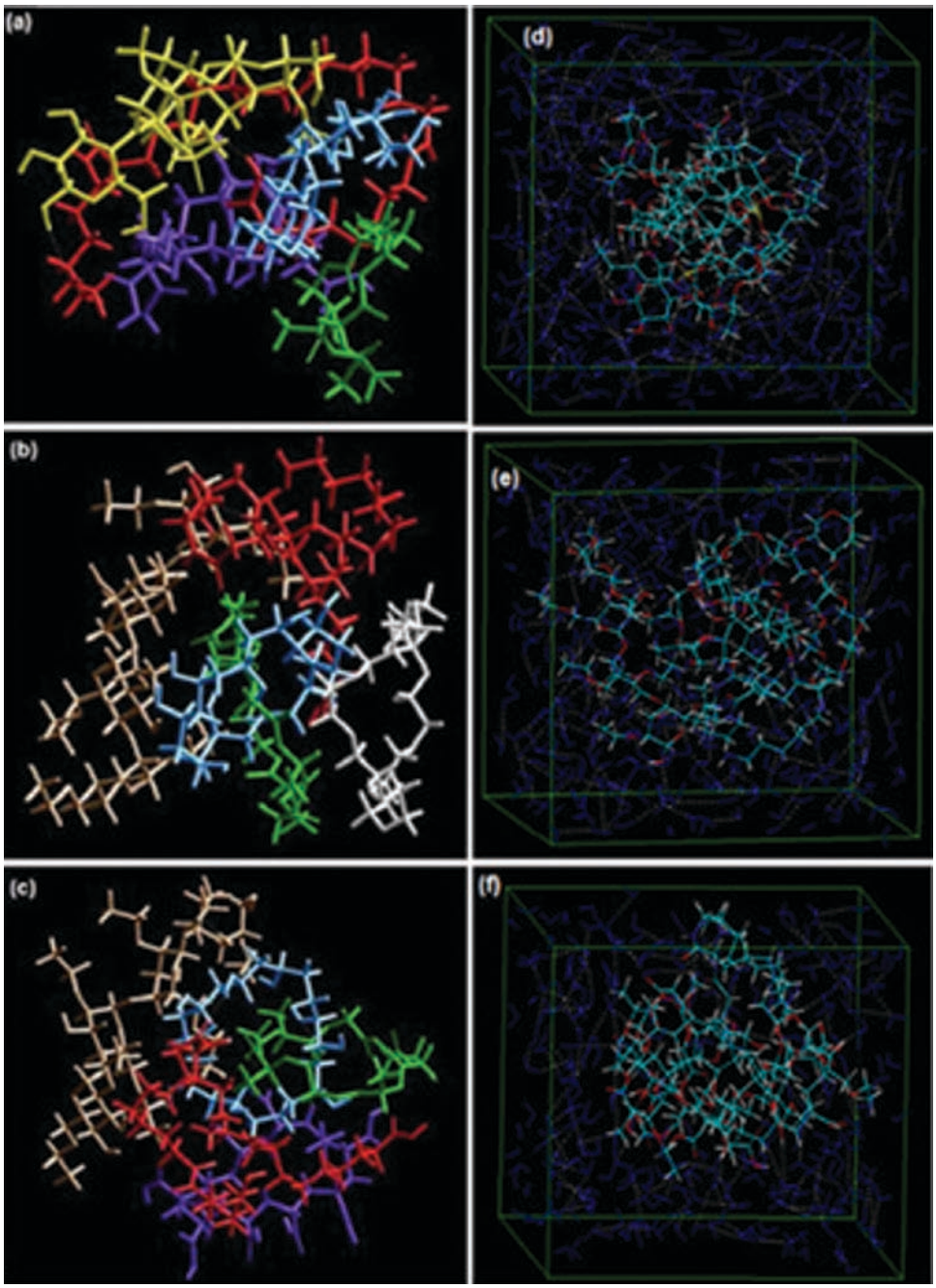

Figure 12. Energy minimized constrained models of the polymeric assemblies derived from molecular mechanics calculations: a) PLGA-mPA6,10-PVA-PAA-Crg, b) PLGA-mPA6,10-PVA-PEO-EC, c) PLGA-mPA6,10-PVA-PAA-EC, d) solvated PLGA-mPA6,10-PVA-PAA-Crg, e) solvated PLGAmPA6,10-PVA-PEO-EC and f) solvated PLGA-mPA6,10-PVA-PAA-EC. Color codes for polymers are: mPA6,10 (red), PLGA (green), PVA (light blue), PAA (violet), CRG (yellow), PEO (white) and EC (brown).

PLGA-mPA6,10-PVA-PAA-EC) and replacing PAA with PEO and EC with CRG. As evident from Table 22, the sequential formation of polymer complexes MPC1, MPC2, MPC 3 and MPC7 were accompanied by energy stabilization, with ΔEbinding of -15.799, -4.047, -22.712 and -52.228, respectively, as compared to the cumulative total of the energy values of the individual polymers and also the preceding polymer assembly. The energy stabilization, ranging between 4.047 kcal/mol (MPC2) and 52.228 kcal/mol (MPC7), confirmed the rationality of this unique polymer blend for the formulation of an IBPD on a molecular level. The energy changes were observed mainly due to van der Waals interactions (due to hydrophobic interactions) followed by bond stretching contributions (reference values were assigned to all of a structure's bond lengths) and bond angle contributions (reference values were assigned to all of a structure's bond angles) and transiently, but importantly, by hydrogen bonds formed due to polymer-polymer interaction in the vacuum Figure 12a–c and polymer-H_2O interaction in the solvated molecules Figure 12d–f. These underlying chemical interactions may cause

Table 21. The selected fifteen lead formulations screened through the OVAT approach.

	Polymeric composition (mg)										
F#	P6	PL	PA	EC	PV	XG	GL	BW	ES	ER	ESR
62	150	400	25	200	25	–	–	–	–	–	0.011
27	200	250	25	300	25	–	–	–	–	–	0.020
51	175	300	25	250	25	–	–	–	25	–	0.023
52	175	300	25	250	25	–	–	–	–	25	0.033
41	175	300	25	250	25	–	25	–	–	–	0.041
39	185	275	25	250	25	40	–	–	–	–	0.044
28	175	250	25	300	50	–	–	–	–	–	0.050
40	180	275	25	250	25	45	–	–	–	–	0.053
44	175	275	25	250	25	50	–	–	–	–	0.060
36	200	275	25	250	25	25	–	–	–	–	0.064
29	150	250	25	300	100	–	–	–	–	–	0.071
50	175	300	25	250	25	–	–	25	–	–	0.073
37	195	275	25	250	25	30	–	–	–	–	0.080
38	190	275	25	250	25	35	–	–	–	–	0.082
31	100	250	25	300	125	–	–	–	–	–	0.084

P6: Modified polyamide 6,10; PL: Poly(lactic–co–glycolic acid); PE: Polyethylene oxide PA: Polyacrylic acid; CG: Carrageenan; EC: Ethycellulose; PV: Polyvinylalcohol; XG: Xanthan gum; GL: gelatin; BW: beeswax; ES: Eudragit S100; ER: Eudragit RS 100; ESR: Equilibrium swelling ratio.

Table 22. Calculated energy parameters (kcal/mol) of the polymeric assemblies between PLGA, $_m$PA6,10, PVA, PAA, PEO, Crg and EC.

	Energy (kcal/mol)						
Structure	Total[a]	$\Delta E_{binding}$ [b]	Bond[c]	Angle[d]	VDW[e]	ΔE_{vdw} [f]	H bond[g]
PLGA	2.020	–	0.523	4.905	–5.982	–	0
PA 6,10	16.959	–	0.824	8.524	–1.154	–	–0.006
PVA	18.517	–	1.068	5.969	4.086	–	–1.818
PAA	29.002	–	2028	19.12	0.133	–	–0.083
PEO	29.483	–	0.644	6.093	7.072	–	0
CRG	284.850	–	6.153	242.054	25.04	–	0
EC	72.116	–	3.552	26.457	8.746	–	–0.209
(MPC1) PLGA–PA6,10	3.180	–15.799	1.345	12.840	–22.873	-15.737	–0.489
(MPC2) PLGA-PA6,10- PVA	33.449	–4.047	6.035	39.596	–24.908	-21.858	–3.042
(MPC3) PLGA-PA6,10-PVA-PAA	43.786	–22.712	7.136	48.463	–60.313	-57.396	–0.120
(MPC4) PLGA-PA6,10-PVA-PEO	57.317	–9.662	6.249	47.421	–33.281	-37.303	–3.488
(MPC5) PLGA-PA6,10-PVA-PEO-EC	106.191	–32.904	9.633	74.394	–43.161	-55.929	–4.126
(MPC6) PLGA-PA6,10-PVA-PAA-Crg	523.872	172.524	103.314	373.429	16.506	-5.617	–3.600
(MPC7) PLGA-PA6,10-PVA-PAA-EC	86.386	–52.228	10.803	76.305	–73.845	-79.674	–0.672
(MPC5-Sol) PLGA-PA6,10-PVA-PEO-EC	–6258.198	–	60.05	129.212	–31.838	–	–18.495
(MPC6-Sol) PLGA-PA6,10-PVA-PAA-Crg	–7337.832	–	164.299	442.012	120.236	–	–16.573
(MPC7-Sol) PLGA-PA6,10-PVA-PAA-EC	–4569.621	–	48.511	116.201	–106.201	–	–15.835

[a]Total steric energy for an optimized structure.
[b]$\Delta E_{binding}$ = E(Host.Guest) – E(Host) – E(Guest).
[c]Bond stretching contributions, reference values were assigned to all of a structure's bond lengths.
[d]Bond angle contributions, reference values were assigned to all of a structure's bond angles.
[e]van der Waals interactions due to non–bonded interatomic distances.
[f]ΔE_{vdw} = Vdw(HostGuest) – VdW(Host) – VdW(Guest).
[g]Hydrogen–bond energy function.

structural changes responsible for high mechanical strength and swelling characteristics of the IBPD. The weak Van der Waals forces may cause aggregation of the aliphatic chains with localized regions having a density and refractive index different from that of the bulk polymers. Additionally, the absence of double bonds, aromatic system and sterically hindered environment in this multi-molecular assembly may further increase the tendency of agglomeration.

Replacement of EC with CRG

The comparative instability of MPC6 with respect to MPC7 (with ΔEbinding difference of 224 kcal/mol) explains the rationale of using EC in place of CRG. EC being a hydrophobic polymer, is stabilized by London dispersion forces (Δevdw = -79.674) which are not so prominent in CRG (Δevdw = +172.524), which is a hydrophilic polymer. These hydrophobic interactions in MPC7 further culminated to form a mechanically tough polymeric complex as

is evident from the increase in bond stretching and bond angle contributions. This significant increase of bond stretching energy and angle bending energy may result in substantial stress development because the ethylcellulose chain with a smaller average molecular weight value may reach its full extension earlier than the carageenan chain, resulting in a higher structural integrity and robustness[83]. This corroborates with the higher longitudinal crushing force of F62 as compared to formulations not containing EC. Conversely, the same is true for CRG where the formulations containing CRG displayed lower mechanical strength due to higher bond stretching and bond angle energies. As expected, the hydrophilic nature of CRG in turn stabilized MPC6-sol under the influence of water molecules in the solvated system whereas the EC containing MPC7-sol displayed stability to hydrolysis due to low water solubility (Table 22). The solvated MPC6-sol-H_2O interaction caused the expansion of the polymer chains in the solvated system and hence the increased bond stretching and bond angle energies Figure 12d–f. Above explanation along with the higher H-bonding and lower van der waals stabilization of solvated MPC6 (-16.573 and 120.236 kcal/mol, respectively) than solvated MPC7 (-15.835 and -106.497 kcal/mol, respectively) clearly explains the minimal swelling capacity or low ESR of F62, thus corroborating the experimental data.

Replacement of PAA with PEO

PAA and PEO, both hydrophilic and bioadhesive polymers, displayed similar total steric energy values (Table 22). Additionally, when incorporated into MPC2, they demonstrated similar bond length and bond angle energy attributes and hence imparting equivalent mechanical strength. However, the hydrophobic interactions, due to van der waals forces, imparted a very different stability profile to the total steric energies of MPC3 and MPC4 with MPC4 stabilized by ~13 kcal/mol as compared to MPC3. The van der waals forces themselves differed by a magnitude of ~20 kcal/mol. These differences were further magnified with the addition of EC to form MPC5 and MPC 7, respectively. The pentapolymeric assemblies thus differed by ~20 and ~24 kcal/mol for $\Delta E_{binding}$ and ΔE_{vdw}, respectively. The above divergence was observed due to more hydrophilic nature of PEO as was evident from the MM simulations in the solvated system wherein MPC5-sol was more stabilized than MPC7-sol under the influence of water molecules Figure 12d–f. In addition, the H-bond energy and the van der waals forces were more equilibrated in case of MPC5-sol and MPC7-sol, respectively (Table 22). The results obtained with CRG once again justified the reluctance of PAA-EC formulations to hydrolysis thus showing a low equilibrium swelling ratio than the PEO-EC formulations, although to a less extent than CRG. The mechanical properties were, however, equivalent even in the solvated system displaying an equivalent polymeric chain expansion. Overall, the above results, i.e. elimination of CRG and addition of EC and elimination of PEO and addition of PAA, may be employed to justify the addition and elimination of other polymeric entities to and from the finalized PLGA-$_m$PA6,10-PVA-PAA-EC (F62) formulation.

Conclusions

Through extensive screening of the developmental formulations using an OVAT approach, coupled with experimental design robust caplets with substantial matrix integrity and desirable drug delivery attributes were produced, as evidenced by the Equilibrium Swelling Ratios, thermal analysis, bioadhesive testing and *in vitro* drug analysis results. This was further evidenced by the chemometric modelling analysis on the IBPD. Fifteen lead formulations with minimal swelling tendencies were obtained. F62 which is composed of $_m$PA 6,10 (150 mg), PLGA (400 mg), EC (200 mg), PVA (25 mg) and PAA (25 mg) appeared to be the most suited in terms of minimal swelling capacity, high matrix stability (including thermal stability), desirable bioadhesivity capacity and the high ability to control the drug release. In synchronizing the experimental and simulation studies, it is quite apparent that apart from equilibrium swelling, the interactions during MPC formations that involved the non-bonded attractive forces, induced dipoles in the complex where the binding energy changes should be proportional to the structural integrity of the polymeric matrix, thus providing a prolonged release of the drug molecules. The drug release may therefore be desirably controlled by increasing and decreasing the proportion of the various polymers used to formulate the IBPD. The molecular mechanics simulations presented in this study may also serve as a template for the inclusion/exclusion/addition/replacement of other polymeric entities for prediction of the compatibility within this unique hydrophobic-hydrophilic polymer engineered intravaginal drug delivery device.

Acknowledgments

This research is supported by the Norwegian Agency for Development Co-operation (NORAD)-NORWAY, and by grants from South African Research Chairs Initiative (SARChI)-National Research Foundation (NRF) of South Africa and the Faculty Research Committee, University of Witwatersrand, Johannesburg, South Africa. St. John's University of Tanzania is sincerely acknowledged. Ethics clearance for this study was obtained from the Animal Ethics Committee of the University of the Witwatersrand (Ethics clearance no. 2007/25/05).

Declaration of interest

The authors declare no interest.

References

1. Garg S, Tambwekar KR. (2003). Development pharmaceutics of microbicide formulations Part II. Formulation, evaluation and challenges. AIDS Patient Care and STDs, 17:377–399.

2. das Neves J, Bahia MF. (2006). Gels as vaginal drug delivery systems. Int J Pharm, 318:1–14.
3. D'Cruz OJ, Uckun FM. (2006). Dawn of non-nucleoside inhibitor-based anti-HIV microbicides. J Antimicrob Chemother, 57:411–423.
4. Andrews GP, Laverty TP, Jones DS. (2009). Mucoadhesive polymeric platforms for controlled drug delivery. Eur J Pharm Biopharm, 71:505–518.
5. Justin-Temu M, Damian F, Kinget R, Van Den Mooter G. (2004). Intravaginal gels as drug delivery systems. J Womens Health (Larchmt), 13:834–844.
6. Ndesendo VM, Pillay V, Choonara YE, Buchmann E, Bayever DN, Meyer LC. (2008). A review of current intravaginal drug delivery approaches employed for the prophylaxis of HIV/AIDS and prevention of sexually transmitted infections. aaps Pharmscitech, 9:505–520.
7. Rohan LC, Sassi AB. (2009). Vaginal drug delivery systems for HIV prevention. Aaps J, 11:78–87.
8. Sekimizu K, Kokudo N. (2008). Dug discoveries and therapeutics, 2, 4, [on line] Available at: http://www.ddtjournal.com/files/DDT_2008Vol2No4_pp200_261.pdf. Accessed on 1 March 2010.
9. Vueba ML, Batista de Carvalho LA, Veiga F, Sousa JJ, Pina ME. (2004). Influence of cellulose ether polymers on ketoprofen release from hydrophilic matrix tablets. Eur j Pharm Biopharm, 58:51–59.
10. Ravi PR, Kotreka UK, Saha RN. (2008). Controlled release matrix tablets of zidovudine: effect of formulation variables on the *in vitro* drug release kinetics. AAPS Pharmscitech, 9:302–313.
11. Siepmann J, Peppas NA. (2001). Modeling of drug release from delivery systems based on hydroxypropyl methylcellulose (HPMC). Adv Drug Deliv Rev, 48:139–157.
12. Avgoustakis K. (2004). Pegylated poly(lactide) and poly(lactide-co-glycolide) nanoparticles: preparation, properties and possible applications in drug delivery. Curr Drug Deliv, 1:321–333.
13. Arifin DY, Lee LY, Wang CH. (2006). Mathematical modeling and simulation of drug release from microspheres: Implications to drug delivery systems. Adv Drug Deliv Rev, 58:1274–1325.
14. Pinto JF, Wunder KF, Okoloekwe A. (2004). Evaluation of the potential use of poly(ethylene oxide) as tablet- and extrudate-forming material. AAPS J, 6:17–26.
15. Hiremath PS, Saha RN. (2008). Oral matrix tablet formulations for concomitant controlled release of anti-tubercular drugs: design and *in vitro* evaluations. Int J Pharm, 362:118–125.
16. Jin X, Zhang Y, Xiao L, Zhao Z. (2008). optimization of extended zero-order release gliclazide tablets using D-optimal mixture design. Yakugaku Zasshi, 128:1475–1483.
17. Hasan EI, Amro BI, Arafat T, Badwan AA. (2003). Assessment of a controlled release hydrophilic matrix formulation for metoclopramide HCl. Eur J Pharm Biopharm, 55:339–344.
18. Chopra S, Patil GV, Motwani SK. (2007). Release modulating hydrophilic matrix systems of losartan potassium: optimization of formulation using statistical experimental design. Eur J Pharm Biopharm, 66:73–82.
19. Rahman BM, Islam MA, Wahed MII, Ahmed M, Islam R, Barman K, Anisuzzaman ASM, Khondkar P. (2009). In vitro studies of pentoxifylline controlled-release from hydrophilic matrices. J Sci Res, 1, 2:353–362.
20. Einmahl S, Capancioni S, Schwach-Abdellaoui K, Moeller M, Behar-Cohen F, Gurny R. (2001). Therapeutic applications of viscous and injectable poly(ortho esters). Adv Drug Deliv Rev, 53:45–73.
21. Breton P, Larras V, Roy D, Sagodira S, Limal D, Bonnafous D et al. (2008). Biocompatible poly(methylidene malonate)-made materials for pharmaceutical and biomedical applications. Eur J Pharm Biopharm, 68:479–495.
22. Barakat NS, Elbagory IM, Almurshedi AS. (2009). Controlled-release carbamazepine matrix granules and tablets comprising lipophilic and hydrophilic components. Drug Deliv, 16:57–65.
23. Nirmal M. (2006). Control release formulation containing a hydrophobic material as the sustained release agent. US Patent, 7052706 [on line] Available at: http://www.patentstorm.us/patents/7052706/description.html. Accessed on 9 June 2009.
24. Khoee S, Hassanzadeh S, Goliaie B. (2007). Effects of hydrophobic drug-polyesteric core interactions on drug loading and release properties of poly (ethylene glycol) triblock core shell nanoparticles. Nanotechnology, 18:1–9.
25. Wu F, Jin T. (2008). Polymer-based sustained-release dosage forms for protein drugs, challenges, and recent advances. aaps Pharmscitech, 9:1218–1229.
26. Smith RC, Leung A, Kim BS, Hammond PT. (2009). Hydrophobic Effects in the Critical Destabilization and Release Dynamics of Degradable Multilayer Films. Chem Mater, 21:1108–1115.
27. Sánchez-Lafuente C, Teresa Faucci M, Fernández-Arévalo M, Alvarez-Fuentes J, Rabasco AM, Mura P. (2002). Development of sustained release matrix tablets of didanosine containing methacrylic and ethylcellulose polymers. Int J Pharm, 234:213–221.
28. Sant S, Thommes M, Hildgen P. (2008). Microporous structure and drug release kinetics of polymeric nanoparticles. Langmuir, 24:280–287.
29. Yu DG, Branford-White C, Ma ZH, Zhu LM, Li XY, Yang XL. (2009). Novel drug delivery devices for providing linear release profiles fabricated by 3DP. Int J Pharm, 370:160–166.
30. Liu J, Zhang F, McGinity JW. (2001). Properties of lipophilic matrix tablets containing phenylpropanolamine hydrochloride prepared by hot-melt extrusion. Eur J Pharm Biopharm, 52:181–190.
31. Tiwari SB, Murthy TK, Pai MR, Mehta PR, Chowdary PB. (2003). Controlled release formulation of tramadol hydrochloride using hydrophilic and hydrophobic matrix system. aaps Pharmscitech, 4:E31.
32. Garg S, Jambu L, Vermani K. (2007). Development of novel sustained release bioadhesive vaginal tablets of povidone iodine. Drug Dev Ind Pharm, 33:1340–1349.
33. Valenta C. (2005). The use of mucoadhesive polymers in vaginal delivery. Adv Drug Deliv Rev, 57:1692–1712.
34. Patel VF, Patel NM. (2007). Statistical evaluation of influence of xanthan gum and guar gum blends on dipyridamole release from floating matrix tablets. Drug Dev Ind Pharm, 33:327–334.
35. Barakat NS, Elbagory IM, Almurshedi AS. (2008). Controlled-release carbamazepine granules and tablets comprising lipophilic and hydrophilic matrix components. aaps Pharmscitech, 9:1054–1062.
36. Sibeko B, Pillay V, Choonara YE, Khan RA, Modi G, Iyuke SE et al. (2009). Computational molecular modeling and structural rationalization for the design of a drug-loaded PLLA/PVA biopolymeric membrane. Biomed Mater, 4:015014.
37. Bettini R, Catellani PL, Santi P, Massimo G, Peppas NA, Colombo P. (2001). Translocation of drug particles in HPMC matrix gel layer: effect of drug solubility and influence on release rate. J Control Release, 70:383–391.
38. Christ KA, Zessin G., Cobet U. (1998). The use of ultrasound and penentrometer to characterize the advancement of swelling and eroding fronts in HPMC matrices. Int J Pharm, 163:123–131.
39. Al-Taani BM, Tashtoush BM. (2003). Effect of microenvironment pH of swellable and erodable buffered matrices on the release characteristics of diclofenac sodium. aaps Pharmscitech, 4:E43.
40. Dahlberg C, Fureby A, Schuleit M, Dvinskikh SV, Furó I. (2007). Polymer mobilization and drug release during tablet swelling. A 1H NMR and NMR microimaging study. J Control Release, 122:199–205.
41. Mehta KA, Kislalioglu MS, Phuapradit W, Malick AW, Shah NH. (2000). Effect of formulation and process variables on porosity parameters and release rates from a multi unit erosion matrix of a poorly soluble drug. J Control Release, 63:201–211.
42. Vlachou M, Naseef H, Efentakis M, Tarantili PA, Andreopoulos AG. (2001). Swelling properties of various polymers used in controlled release systems. J Biomater Appl, 15:293–306.
43. Haltrich D, Lavssamayer B, Steiner W. (1994). Xylanase formation by Sclerotium rolfsii effect of growth substrates and development of a culture medium using statistical designed experiments. Appl Microbiol Biotechnol 42:522–530.
44. He GQ, Chen QH, Ju XJ, Shi ND. (2004). Improved elastase production by Bacillus sp. EL31410–further optimization and kinetics studies of culture medium for batch fermentation. J Zhejiang Univ Sci, 5:149–156.

45. Kolawole OA, Pillay V, Choonara YE. (2007). Novel polyamide 6,10 variants Synthesized by modified interfacial polymerization for application as a rate-modulated monolithic drug delivery System. J Bioact Compat Pol, 22:281–313.
46. D'Cruz OJ, Uckun FM. (2002). Pre-clinical safety evaluation of novel nucleoside analogue-based dual-function microbicides (WHI-05 and WHI-07). J Antimicrob Chemother, 50: 793–803.
47. Zhang H, Dornadula G, Beumont M, Livornese L Jr, Van Uitert B, Henning K et al. (1998). Human immunodeficiency virus type 1 in the semen of men receiving highly active antiretroviral therapy. n Engl J Med, 339:1803–1809.
48. Garg S, Verman K, Anderson RA, Zaneveld LJ. (2004). Rapidly disintegrating novel bioadhesive vaginal tablets of polystyrene sulfonate (PSS), a potential microbicide formulation. International Conference of AIDS. Abstract No. TuPeB4656 [on line] Available at: http://gateway.nlm.nih.gov/MeetingAbstracts/ma?f=102282478.html. Accessed on 12 November 2007.
49. Richardson BA, Martin HL Jr, Stevens CE, Hillier SL, Mwatha AK, Chohan BH et al. (1998). Use of nonoxynol-9 and changes in vaginal lactobacilli. J Infect Dis, 178:441–445.
50. Rosenstein IJ, Stafford MK, Kitchen VS, Ward H, Weber JN, Taylor-Robinson D. (1998). Effect on normal vaginal flora of three intravaginal microbicidal agents potentially active against human immunodeficiency virus type 1. J Infect Dis, 177: 1386–1390.
51. Anderson RA, Feathergill K, Diao X, Cooper M, Kirkpatrick R, Spear P et al. (2000). Evaluation of poly(styrene-4-sulfonate) as a preventive agent for conception and sexually transmitted diseases. J Androl, 21:862–875.
52. Simoes JA, Citron DM, Aroutcheva A, Anderson RA Jr, Chany CJ 2nd, Waller DP et al. (2002). Two novel vaginal microbicides (polystyrene sulfonate and cellulose sulfate) inhibit Gardnerella vaginalis and anaerobes commonly associated with bacterial vaginosis. Antimicrob Agents Chemother, 46:2692–2695.
53. Buddhikot M, Falkenstein E, Wehling M, Meizel S. (1999). Recognition of a human sperm surface protein involved in the progesterone-initiated acrosome reaction by antisera against an endomembrane progesterone binding protein from porcine liver. Mol Cell Endocrinol, 158:187–193.
54. Quintanar-Guerrero D, Villalobos-García R, Alvarez-Colín E, Cornejo-Bravo JM. (2001). *In vitro* evaluation of the bioadhesive properties of hydrophobic polybasic gels containing N,N-dimethylaminoethyl methacrylate-co-methyl methacrylate. Biomaterials, 22:957–961.
55. Sandri G, Rossi S, Ferrari F, Bonferoni MC, Muzzarelli C, Caramella C. (2004). Assessment of chitosan derivatives as buccal and vaginal penetration enhancers. Eur J Pharm Sci, 21:351–359.
56. D'Cruz OJ, Erbeck D, Uckun FM. (2005). A study of the potential of the pig as a model for the vaginal irritancy of benzalkonium chloride in comparison to the nonirritant microbicide PHI-443 and the spermicide vanadocene dithiocarbamate. Toxicol Pathol, 33:465–476.
57. Owen DH, Katz DF. (2005). A review of the physical and chemical properties of human semen and the formulation of a semen simulant. J Androl, 26:459–469.
58. Owen DH, Katz DF. (1999). A vaginal fluid simulant. Contraception, 59:91–95.
59. Campo VL, Kawano DF, da Silva DB, Carvalho I. (2009). Carrageenans: Biological properties, chemical modifications and structural analysis – A review. Carbohydr. Polym, 77:167–180.
60. Varma M, Singla AK, Dhawan S. (2004). Release of diltiazem hydrochloride from hydrophilic matrices of polyethylene oxide and carbopol. Drug Dev Ind Pharm, 30:545–553.
61. Yan C, Wu G, Lin S. (2006). Alkaline blend polymer electrolytes based on polyvinyl alcohol (PVA)/tetraethyl ammonium chloride (TEAC). J Appl Electrochem, 36:655–661.
62. Yang Y, Liu C, Wu H. (2008). Preparation and properties of poly(vinyl alcohol)/exfoliated α-zirconium phosphate nanocomposite films. Polym. Test, 28:371–377.
63. Mukherjee GS. (2009). Calorimetric characterization of membrane materials based on polyvinyl alcohol. J Therm Anal Calorim, 96:21–25.
64. Rodd AB, Dunstan DE, Boger DV. (2000). Characterisation of xanthan gum solutions using dynamic light scattering and rheology. Carbohydr Polym, 42, 159–174.
65. Iseki T, Takahashi M, Hattori H, Hatakeyama T, Hatakeyama H. (2001). Viscoelastic properties of xanthan gum hydrogels annealed in the sol state. Food and Hydrocolloids, 15:503–506.
66. Quinn FX, Hatakeyama T, Takahashi M, Hatakeyama H. (1994). The effect of annealing on the conformational properties of xanthan hydrogels. Polymer, 35:1248–1252.
67. Song K, Kim Y, Chang G. (2006). Rheology of concentrated xanthan gum solutions: Steady shear flow behavior. Fibers and Polymers, 7, 129–138.
68. Soukoulis C, Panagiotidis P, Koureli R, Tzia C. (2007). Industrial yogurt manufacture: monitoring of fermentation process and improvement of final product quality. J Dairy Sci, 90: 2641–2654.
69. Billa N, Yuen KH. (2000). Formulation variables affecting drug release from xanthan gum matrices at laboratory scale and pilot scale. AAPS Pharmscitech, 1:E30.
70. Ward G, Courts A. (1977). The science and technology of gelatin. London; New York: Academic Press, 1977 [on line] Available at: http://catalogue.nla.gov.au/Record/828694. Accessed on 24 August 2009.
71. Baumgartner S, Kristl J, Peppas NA. (2002). Network structure of cellulose ethers used in pharmaceutical applications during swelling and at equilibrium. Pharm Res, 19:1084–1090.
72. Pignatello R, Bucolo C, Ferrara P, Maltese A, Puleo A, Puglisi G. (2002). Eudragit RS100 nanosuspensions for the ophthalmic controlled delivery of ibuprofen. Eur J Pharm Sci, 16:53–61.
73. Ndesendo VM, Meixner W, Korsatko W, Korsatko-Wabnegg B. (1996). Microencapsulation of chloroquine diphosphate by Eudragit RS100. j Microencapsul, 13:1–8.
74. Wong CF, Yuen KH, Peh KK. (1999). Formulation and evaluation of controlled release Eudragit buccal patches. Int J Pharm, 178:11–22.
75. Trapani A, Laquintana V, Denora N, Lopedota A. (2007). Eudragit RS 100 microparticles containing 2-hydroxypropyl-β-cyclodextrin and glutathione: Physicochemical characterization, drug release and transport studies. Eur J Pharm Sci, 30:64–74.
76. Umamaheshwari RB, Ramteke S, Jain NK. (2004). Anti–Helicobacter Pylori Effect of Bioadhesive Nanoparticles Bearing Amoxicillin in Experimental Gerbils Model. AAPS Pharm Sci Tech, 5:2.
77. Ndesendo VM, Pillay V, Choonara YE, Khan RA, Meyer L, Buchmann E et al. (2009). *In vitro* and ex vivo bioadhesivity analysis of polymeric intravaginal caplets using physicomechanics and computational structural modeling. Int J Pharm, 370:151–159.
78. Gimeno E, Moraru CI, Kokini JL. (2003) Effects of Xanthan gum and CMC on the structure and texture of corn flour pellets expanded by microwave heating. Cereal Chem, 81:100–107.
79. Guoqiang D, Batra R, Kaul R, Gupta MN, Mattiasson B. (1995). Alternative modes of precipitation of Eudragit S 100: a potential ligand carrier for affinity precipitation of protein. Bioseparation, 5:339–350.
80. Arasaratnam V V, Galaev IY, Mattiasson B. (2000). Reversibly soluble biocatalyst: optimization of trypsin coupling to Eudragit S-100 and biocatalyst activity in soluble and precipitated forms. Enzyme Microb Technol, 27:254–263.
81. Girish KL, Dhiren PS. (2008). Evaluation of Mucilage of Hibiscus rosasinensis Linn as Rate Controlling Matrix for Sustained Release of Diclofenac. Drug Dev Ind Pharm, 34:807–816.
82. Wen X, Wang T, Wang Z, Li L, Zhao C. (2008). Preparation of konjac glucomannan hydrogels as DNA-controlled release matrix. Int J Biol Macromol, 42:256–263.
83. Jang SS, Goddard WA. (2007). Mechanical and Transport Properties of the Poly(ethylene oxide)-Poly(acrylic acid) Double Network Hydrogel from Molecular Dynamic Simulations. J Phys Chem B, 111:1729–1737.